Environmental Toxicology

Influence of Species-Specific Feeding Ecology on Mercury Concentrations in Seabirds Breeding on the Chatham Islands, New Zealand

Justine Thébault,[a,b,*] Paco Bustamante,[b,c] Melanie Massaro,[d] Graeme Taylor,[e] and Petra Quillfeldt[a]

[a]Department of Animal Ecology and Systematics, Justus Liebig University Giessen, Giessen, Germany
[b]Littoral Environnement et Sociétés (LIENSs), UMR 7266 CNRS–La Rochelle Université, La Rochelle, France
[c]Institut Universitaire de France (IUF), Paris, France
[d]Institute for Land, Water and Society, School of Environmental Sciences, Charles Sturt University, Albury, Australia
[e]Department of Conservation, Biodiversity Group, Wellington, New Zealand

Abstract: Mercury (Hg) is a toxic metal that accumulates in organisms and biomagnifies along food webs; hence, long-lived predators such as seabirds are at risk as a result of high Hg bioaccumulation. Seabirds have been widely used to monitor the contamination of marine ecosystems. In the present study, we investigated Hg concentrations in blood, muscle, and feathers of 7 procellariform seabirds breeding on the Chatham Islands, New Zealand. Using bulk and compound-specific stable isotope ratios of carbon and nitrogen as a proxy of trophic position and distribution, we also tested whether Hg contamination is related to the species-specific feeding ecology. Mercury exposure varied widely within the seabird community. The highest contaminated species, the Magenta petrel, had approximately 29 times more Hg in its blood than the broad-billed prion, and approximately 35 times more Hg in its feathers than the grey-backed storm petrel. Variations of Hg concentrations in blood and feathers were significantly and positively linked to feeding habitats and trophic position, highlighting the occurrence of efficient Hg biomagnification processes along the food web. Species and feeding habitats were the 2 main drivers of Hg exposure within the seabird community. The *Pterodroma* species had high blood and feather Hg concentrations, which can be caused by their specific physiology and/or because of their foraging behavior during the interbreeding period (i.e., from the Tasman Sea to the Humboldt Current system). These 2 threatened species are at risk of suffering detrimental effects from Hg contamination and further studies are required to investigate potential negative impacts, especially on their reproduction capability. *Environ Toxicol Chem* 2021;40:454–472. © 2020 The Authors. *Environmental Toxicology and Chemistry* published by Wiley Periodicals LLC on behalf of SETAC.

Keywords: Heavy metal; Bioaccumulation; Food web; Bulk stable isotopes; Compound-specific isotopic analyses of amino acids; *Pterodroma*

INTRODUCTION

Mercury (Hg) is a toxic and pervasive metal that occurs naturally in the environment; it is emitted from topsoil, volcanoes, and other geothermal sources (Pirrone et al. 2010).

However, anthropogenic activities have substantially modified the cycling of this trace element on a global scale, mainly through the combustion of fossil fuels, industrial and agricultural pollution, waste incineration, and gold mining (Eagles-Smith et al. 2018). In combination, these human-induced perturbations are currently responsible for two-thirds of the global Hg emissions (Pacyna et al. 2006). Mercury is non-essential and can lead—even at low doses—to broad deleterious effects in biota by altering the functioning of the nervous, reproductive, and immune systems (Wolfe et al. 1998; Tan et al. 2009). The elemental form of this metal (Hg^0) is highly volatile and has a long atmospheric residence time of approximately 1 yr (Saiz-Lopez et al. 2018). Consequently, it is transported by atmospheric winds over long

distances across the globe, and high concentrations of Hg can also be found in remote environments (Fitzgerald et al. 1998).

In marine ecosystems, which are known to be major repositories of environmental contaminants, anthropogenic emissions have tripled the Hg concentrations in surface waters compared with those before the Anthropocene (Lamborg et al. 2014). The key source of Hg in the ocean is the atmospheric deposition of its inorganic form (Hg^{II}; Fitzgerald et al. 2007). In the water column, biotic and abiotic reactions contribute to Hg^{II} turning into other chemical forms of Hg. For instance, reactions with microorganisms can lead to the methylation of Hg (Hsu-Kim et al. 2013; Villar et al. 2020) to form methylmercury (MeHg), one of the most toxic species of Hg because of its high bioavailability and affinity for proteins (Rabenstein 1978a, 1978b). In this organic form, Hg accumulates in organisms over time and biomagnifies along food webs; thus, predators exhibit higher concentrations than their prey (Dietz et al. 2000).

Because seabirds are long-lived mesopredators or top predators, they accumulate high levels of Hg; hence, they have been widely used as sentinels for monitoring contamination in marine food webs (e.g., Gilbertson et al. 1987; Burger 1993; Monteiro and Furness 1995; Blévin et al. 2013; Carravieri et al. 2016). Mercury contamination in seabirds occurs mainly via food intake (Atwell et al. 1998; Burger and Gochfeld 2004), and because Hg is not homogeneously distributed in marine ecosystems (Monteiro et al. 1996; Choy et al. 2009; Blum et al. 2013), trophic ecology has been proven to be the main driver of intra- and inter-species variations of Hg concentrations (Bearhop et al. 2000a; Anderson et al. 2009; Carravieri et al. 2014a). For example, Hg bioaccumulation is enhanced in the mesopelagic zone as a result of high levels in prey (Monteiro et al. 1996; Chouvelon et al. 2012) and water chemistry controlling Hg speciation and uptake at the base of the food webs (Lavoie et al. 2013; Renedo et al. 2020). Furthermore, despite the poleward increase of Hg concentrations in surface waters (Cossa et al. 2011), previous studies in the Southern Ocean have reported higher Hg levels in seabirds foraging in subtropical waters than in seabirds foraging in sub-Antarctic and Antarctic waters (e.g., Carravieri et al. 2014b, 2017, 2020a; Cherel et al. 2018). This unexpected pattern has been attributed to the higher complexity, and thus Hg biomagnification, of food webs at lower latitudes (Carravieri et al. 2017).

When seabirds forage on contaminated prey, Hg is absorbed through the digestive tract and transported via the bloodstream to internal tissues where it is stored, mainly into the liver, kidneys and muscles (Walker et al. 2012). Stored MeHg can be remobilized into the circulatory system at a later time and excreted into the growing feathers during the moult (Furness et al. 1986; Renedo et al. 2021). Feathers are inert and preserve their chemical signature when completely grown (Inger and Bearhop 2008). The principal route of Hg excretion in most seabird species is thought to be through the feathers (Monteiro and Furness 1995), reflecting long-term Hg exposure (Braune and Gaskin 1987; Albert et al. 2019). Recent investigation, however, documented a significant influence of recent food intake on feather Hg concentrations in some seabird

groups (e.g., albatrosses; Cherel et al. 2018). In contrast, Hg concentrations in blood provide information about short-term Hg exposure (some weeks–a few months; Monteiro and Furness 2001). Nearly all Hg in blood, feathers, and muscle of seabirds is present in the form of MeHg (Thompson et al. 1990; Bond and Diamond 2009; Renedo et al. 2017); accordingly, total Hg concentration is often used as a proxy for this highly bioavailable chemical form, and will hereafter be referred as Hg concentration.

Among seabirds, Procellariiformes display a wide range of trophic positions—from zooplankton-eaters to apex predators—and feed in different habitats over a large latitudinal gradient (Croxall and Prince 1980; Anderson et al. 2009). Procellariiformes are therefore ideal models for the assessment of Hg biomagnification in marine food webs. Earlier studies have reported very large Hg contamination levels within this order that were explained by diet and feeding habitat (Becker et al. 2002; Bocher et al. 2003; Anderson et al. 2009; Carravieri et al. 2014a, 2014b; Cherel et al. 2018). A recent investigation found elevated Hg concentrations in the feathers of grey-faced petrel (*Pterodroma gouldi*) breeding in northern New Zealand (Lyver et al. 2017), similar to the levels detected in albatrosses, which are known to have the highest Hg levels recorded for any bird group (Cherel et al. 2018). Nevertheless, little data about Hg concentrations in seabird tissues are available in the literature for this region (Lock et al. 1992; Stewart et al. 1999; Lyver et al. 2017).

The aim of the present study was to document Hg concentrations in blood, muscle, and feathers of adult seabirds belonging to 7 procellariform species breeding sympatrically in the Chatham Islands, New Zealand. We examined the influence of feeding ecology on Hg exposure using bulk stable isotope ratios of carbon ($\delta^{13}C$) as a proxy of the feeding habitat, and bulk stable isotope ratios of nitrogen ($\delta^{15}N$) and compound-specific isotopic analyses of amino acids (CSIA-AA) as proxies of the trophic position. Seabird $\delta^{13}C$ signatures indicate their latitudinal feeding grounds and depict neritic versus oceanic foragers (Cherel and Hobson 2007; Jaeger et al. 2010), whereas $\delta^{15}N$ values increase with trophic position (DeNiro and Epstein 1981; McClelland and Montoya 2002; Cherel et al. 2010). In addition, we tested the influence of Hg concentrations on stress levels via the determination of white blood cell profiles on blood smears. Acute or chronic stress can influence white blood cell profiles of individuals, notably the number of leucocytes or the heterophil:lymphocyte ratios that reflect immune status in birds (Vleck et al. 2000). Individuals experiencing stress exhibit higher heterophil:lymphocyte ratios (Gross and Siegel 1983). The determination of heterophil:lymphocyte ratios is broadly used to study immune status in birds; however, this method has not been tested yet to evaluate a potential Hg-induced immuno-modulation.

Considering that the species investigated present distinct foraging strategies, we made the following 4 predictions. 1) Because Hg biomagnifies along food webs, seabird Hg concentrations should be positively correlated to their trophic positions. 2) Given that Hg is not homogeneously distributed in the ocean, seabirds feeding on mesopelagic prey should be

TABLE 1: Foraging habitats and main prey types consumed by the Chatham Islands seabird species included in the present study

Species	Abbreviation	Foraging habitat (horizontal)	Foraging habitat (vertical)	Main prey types	References
Broad-billed prion (*Pachyptila vittata*)	BBP	Neritic, oceanic	Epipelagic	Crustaceans	Imber (1981), Richdale (1944), Klages and Cooper (1992), Grecian et al. (2016)
Chatham petrel (*Pterodroma axillaris*)	CHPE	Oceanic	Epipelagic	Cephalopods, fishes	Heather and Robertson (2005), BirdLife International (2018a)
Common diving petrel (*Pelecanoides urinatrix*)	CODP	Neritic	Epipelagic	Crustaceans	Payne and Prince (1979), Ridoux (1994), Reid et al. (1997), Bocher et al. (2000a, 2001), Schumann et al. (2008)
Grey-backed storm petrel (*Garrodia nereis*)	GBSP	Neritic	Epipelagic	Crustaceans	Imber (1981), Ridoux (1994)
Magenta petrel (*Pterodroma magentae*)	MAPE	Oceanic	Epipelagic and mesopelagic	Cephalopods, fishes	Heather and Robertson (2005), BirdLife International (2018b), Taylor (unpublished data)
Sooty shearwater (*Ardenna grisea*)	SOSH	Oceanic, neritic	Epipelagic	Crustaceans, cephalopods, fishes	Cruz et al. (2001), Kitson et al. (2000)
White-faced storm petrel (*Pelagodroma marina*)	WFSP	Oceanic, neritic	Epipelagic	Fishes, crustaceans	Imber (1981), Spear and Ainley (2007)

more contaminated than seabirds feeding on epipelagic prey, and species foraging at lower latitudes are expected to be exposed to higher Hg levels. 3) *Pterodroma* petrels are oceanic and rely extensively on mesopelagic fish and cephalopods that are enriched in MeHg (Monteiro et al. 1996; Bustamante et al. 2006). *Pterodroma* petrels from other regions of the world were found to have high Hg levels (Carravieri et al. 2014a). Accordingly, we predicted that the *Pterodroma* petrels in the present study have the highest Hg concentrations among the Chatham Islands seabird community. 4) Finally, high blood Hg concentrations should be associated with an increased stress level; therefore, we expected a species-specific positive correlation between Hg concentrations and heterophil:lymphocyte ratios and/or number of leucocytes.

MATERIALS AND METHODS

Study area, species, and sample collection

All fieldwork was carried out in 2015 at 2 different sites in the Chatham Islands, New Zealand: the Tuku (southern part) of the main Chatham Island (Rekohu/Wharekauri 44°04′S, 176°36′W), and on South East Island (Hokorereoro/Rangatira 44°20′S, 176°10′W). We collected samples of the Magenta petrel (*Pterodroma magentae*), a New Zealand endemic species also known as the Chatham Island Taiko, in the Tuku from the end of September to mid-October. The Magenta petrel is one of the world's rarest seabirds with an estimated population size of 150 to 200 birds, including only 80 to 100 mature individuals (Taylor et al. 2012). On South East Island, we sampled 6 breeding seabird species from November to December: broad-billed prion (*Pachyptila vittata*), Chatham petrel (*Pterodroma axillaris*), common diving petrel (*Pelecanoides urinatrix*), grey-backed storm petrel (*Garrodia nereis*), sooty shearwater (*Ardenna grisea*) and white-faced storm petrel (*Pelagodroma marina*). These species feed on a broad diversity of prey types and use contrasting feeding habitats (Table 1).

Adult birds were generally captured by hand in the colony when arriving from foraging after nightfall, except for Magenta petrels that were captured during daylight hours within their artificial breeding burrows. All birds were released at the location of capture immediately after sampling. Blood and feather samples were collected for 7 to 11 individuals per species. Body feathers were plucked and conserved in sealed plastic bags until analysis. Measurements were performed on body feathers that are commonly considered as the best feather type to collect because they are more representative of the entire plumage than other feather types and more homogeneous (Furness et al. 1986). Body feathers were sampled on the flank for broad-billed prion, Magenta petrel, and white-faced storm petrel, and under the tail for Chatham petrel, common diving petrel, grey-backed storm petrel, and sooty shearwater. Blood samples were collected from the brachial vein with a capillary after puncture with a needle. Whole blood was centrifuged and red blood cells—in which Hg preferentially partitions (Tavares et al. 2013)—were used to perform the analyses. Whole blood and blood cells display very similar isotopic signatures (Cherel et al. 2005). In addition, broad-billed prion and white-faced storm petrel muscle was sampled from individuals found dead, trapped in the vegetation. Blood and muscle samples were stored at –20 °C before the analyses. Mercury and bulk stable isotope analyses were performed on the same samples. Compound-specific isotopic analyses of amino acids require a substantial sample mass (~4 mg); therefore, whenever possible, analyses were performed on the same samples as the Hg and bulk stable isotope analyses; if those samples were not substantial enough, samples from other individuals were analyzed.

Preparation of the samples

One body feather per individual was analyzed for Magenta petrels. For the other species, between 2 and 4 feathers were

pooled per individual. Pooling feathers limits potential differences in trace element concentrations among feathers of the same individual. To remove surface contaminants, feathers of each individual were separately cleaned in a chloroform:methanol solution (2:1, v/v; after cutting off the calamus and afterfeather), placed in an ultrasonic bath for 3 min, and rinsed in 2 successive baths of methanol. Feathers were then oven-dried for 48 h at 45 °C and cut into tiny fragments with stainless steel scissors to obtain a homogenous powder. Blood cells and muscle samples were freeze-dried and ground into a fine powder with a spatula and stainless steel scissors. Preparation of the samples as well as Hg and bulk stable isotope analyses were performed at the University of La Rochelle in France, whereas CSIA-AA were conducted at the University of California Davis Stable Isotope Facility, Davis, CA, USA.

Bulk stable isotope analyses

Lipids are impoverished in ^{13}C compared with other tissue components (DeNiro and Epstein 1977). To allow comparison of $\delta^{13}C$ values among species and individuals without detrimental impact of potential variable lipid contents, fat extraction was conducted on muscle samples using cyclohexane as described in Chouvelon et al. (2011). Similar to feathers, blood has consistently low ratios of mass percentages in C and N (C:N < 4.0; Post et al. 2007) because of low lipid content. Thus, these tissues do not require lipid extraction (Bearhop et al. 2000b).

To perform stable isotope analyses, 0.2 to 0.4 mg of subsample were weighed in tin cups. Carbon and nitrogen ratios were determined with a continuous-flow mass spectrometer (Thermo Scientific Delta V Advantage) coupled with an elemental analyzer (Thermo Scientific Flash EA 1112). Measurements of internal laboratory standards were conducted using acetanilide and peptone and indicated an experimental precision of ±0.15 ‰ for both elements. Results are expressed in parts per thousand (‰) in the usual δ notation, relative to Vienna Pee Dee Belemnite for $\delta^{13}C$ and atmospheric N_2 for $\delta^{15}N$, according to Equation 1.

$$\delta^{13}C \text{ or } \delta^{15}N = \left(\frac{R_{sample}}{R_{standard}} - 1 \right) \times 10^3 \qquad (1)$$

where R is $^{13}C/^{12}C$ or $^{15}N/^{14}N$, respectively.

CSIA-AA

Compound-specific isotopic analyses of amino acids methods are based on the absence of change in $\delta^{15}N$ values of some amino acids between a prey and its consumer (source amino acids; e.g., phenylalanine), whereas other amino acids display consistently large increases (trophic amino acids; e.g., glutamic acid). When compared with bulk isotopic analysis, the 2 main interests of the approaches are: 1) the quantification of both baseline and trophic $\delta^{15}N$ values on the same consumer tissue sample, and 2) the relative estimation of trophic position

of consumers by subtracting baseline to trophic $\delta^{15}N$ values. Despite the great advantages of this technique, few studies have yet used it to study the influence of foraging ecology on Hg concentrations in seabirds (Elliott and Elliott 2016; Gagné et al. 2019; Carravieri et al. 2020b).

Linear models derived from CSIA-AA were used to determine more precise trophic positions than bulk $\delta^{15}N$ values can provide. These linear models also cope better with ^{15}N baseline variations among ecosystems (McClelland and Montoya 2002).

Compound-specific isotopic analyses of amino acids were carried out according to Walsh et al. (2014) and Yarnes and Herszage (2017) using a Thermo GC-C-IRMS system composed of a Trace Ultra GC gas chromatograph (Thermo Electron) coupled with a Delta V Plus isotope ratio mass spectrometer through GC IsoLink interface (Thermo Electron). Compound identification support was provided by a Varian CP3800 gas chromatograph coupled with a Saturn 2200 ion trap MS/MS (Varian). Proteins were hydrolyzed in a subsample of approximately 4 mg with 6 M HCl during 70 min at 150 °C, under N_2 headspace, which enabled their chromatographic separation in a DB-23 (Agilent Technologies) column (30 m, 0.25-mm outer diameter [OD], 0.25-mm film; constant flow 1.6 mL/min). The derivatives were methoxycarbonyl amino acid methyl esters. Each compound was then combusted at 1000 °C with Ni/NiO/CuO catalyst and introduced into the isotope ratio mass spectrometer. Laboratory standard measurements, previously calibrated against National Institute of Standards and Technology Standard Reference Materials, indicated standard deviations of <0.3 ‰ for $\delta^{13}C$ and $\delta^{15}N$ values. Laboratory reference materials and expected values were bovine liver ($\delta^{13}C$ = –21.7 ‰; $\delta^{15}N$ = 7.7 ‰), USGS-41 glutamic acid ($\delta^{13}C$ = 37.6 ‰; $\delta^{15}N$ = 47.6 ‰), Nylon5 ($\delta^{13}C$ = –27.7 ‰; $\delta^{15}N$ = –10.3 ‰), and glutamic acid ($\delta^{13}C$ = –16.7 ‰; $\delta^{15}N$ = –6.8 ‰). Specifically, standard deviations in the analytical run for the reference standards were 0.12 ($\delta^{13}C$) and 0.08 ($\delta^{15}N$) for bovine liver; 0.24 ($\delta^{13}C$) and 0.09 ($\delta^{15}N$) for USGS-41 glutamic acid; 0.15 ($\delta^{13}C$) and 0.13 ($\delta^{15}N$) for Nylon5; and 0.05 ($\delta^{13}C$) and 0.24 ($\delta^{15}N$) for glutamic acid. Five samples per tissue were analyzed for each species.

The calculation of the trophic position with CSIA-AA (TP$_{CSIA}$) differed from Quillfeldt et al. (2017) for 3 reasons. 1) In that paper only feathers were analyzed. 2) The formula used by Quillfeldt et al. (2017) was derived from a source with a typographical error (Equation 2 in McMahon et al. 2015) and thus had to be corrected in the present study. 3) More specific trophic discrimination factor (TDF) values have become available. Trophic positions derived from CSIA-AA are hereafter referred to as TP$_{CSIA}$.

Trophic positions derived from CSIA-AA were calculated from the nitrogen stable isotope values of glutamic acid (Glx, i.e. glutamic acid and glutamine) and phenylalanine (Phe; Chikaraishi et al. 2009), using a multi-trophic discrimination factor approach, which accounts for the fact that TDF$_{Glx-Phe}$ is not constant across all trophic positions (e.g., Hoen et al. 2014). We applied a TDF$_{Glx-Phe}$ for plankton of 6.2 ‰ (McMahon and McCarthy 2016). In birds, lower TDF values have recently been found: 3.5 ‰ for feathers of

458

Environmental Toxicology and Chemistry, 2021;40:454–472—J. Thébault et al.

Gentoo penguins (McMahon et al. 2015), and 4.1‰ for muscle of American kestrels (Hebert et al. 2016). To analyze seabird feathers and muscle, it would therefore seem appropriate to use a multi-TDF$_{Glx\text{-}Phe}$ (Hoen et al. 2014; Equations 2 and 3), where 6.2‰ is the overall mean TDF across a wide range of taxa, diet types, and modes of nitrogen excretion (McMahon and McCarthy 2016), 3.5 or 4.1‰ is the TDF for seabird feathers or bird muscle, respectively, and 3.4‰ is the difference in $\delta^{15}N$ values between glutamic acid and phenylalanine in primary producers (plankton).

$$TP_{CSIA}[\text{feathers}] = 2 + \frac{Glx - Phe - 3.5‰ - 3.4‰}{6.2‰} \quad (2)$$

$$TP_{CSIA}[\text{muscle}] = 2 + \frac{Glx - Phe - 4.1‰ - 3.4‰}{6.2‰} \quad (3)$$

For red blood cells, we applied a TDF of 4‰ (Equation 4).

$$TP_{CSIA}[\text{blood}] = 2 + \frac{Glx - Phe - 4‰ - 3.4‰}{6.2‰} \quad (4)$$

This value was derived from a comparison of the TP_{CSIA} values of feathers and red blood cells grown at the same time in thin-billed prion chicks for different TDF values (Quillfeldt and Masello 2020), given that both tissues should reflect the same trophic position of the birds, and a similar time frame of 2 to 4 wk (Quillfeldt et al. 2008). Undertail covert feathers are 50 to 60 mm in length and take approximately the same time to grow (Quillfeldt and Masello 2020).

Calculation of trophic positions from linear regression models

The marine baseline $\delta^{15}N$ ratio can be influenced by factors such as latitude and primary productivity, and change over time (Post 2002; McMahon et al. 2013). However, ecotoxicological studies frequently use $\delta^{15}N$ values to compare populations foraging across large geographic scales without considering disparities in baseline values between food webs (Brasso and Polito 2013). In the Southern Hemisphere, a latitudinal enrichment in $\delta^{15}N$ baseline values occurs from the Antarctic to the subtropical waters, potentially resulting in a bias when using raw $\delta^{15}N$ values to compare the diet of species foraging in different habitats (Jaeger et al. 2010).

A substantial spread was observed in looking at the relationship between 2 indicators of the trophic position in blood, muscle, and feather samples (bulk $\delta^{15}N$ and TP_{CSIA}); this was potentially caused by the fact that the seabird species investigated feed across large geographic scales. In the present study, to address this bias we proposed to calculate the trophic positions of the birds by applying linear regression models to study the relationship between TP_{CSIA} and bulk stable isotope values ($\delta^{13}C$ and $\delta^{15}N$). Trophic positions calculated with linear models are hereafter referred to as TP_{LM}. Raw $\delta^{15}N$ values and TP_{LM} will be compared in their ability to explain variations of Hg concentrations in seabirds.

Linear regression models were used to study the relationship between TP_{CSIA} and bulk stable isotope values ($\delta^{13}C$ and $\delta^{15}N$). Models were applied separately for blood and muscle samples, both reflecting short-term food intake and having similar TDF (Hebert et al. 2016; Quillfeldt and Masello 2020) and for feather samples, providing information about the trophic ecology at the time of the moult. Equations 5 and 6 were derived from these linear models.

$$TP_{LM}[\text{blood, muscle}] = -0.4298 - 0.1441 \times \delta^{13}C + 0.1189 \times \delta^{15}N \quad (5)$$

$$TP_{LM}[\text{feathers}] = 1.2990 - 0.0962 \times \delta^{13}C + 0.0671 \times \delta^{15}N \quad (6)$$

These equations were then used to calculate trophic positions for all samples, using bulk stable isotope values. Detailed information regarding the calculation of trophic positions from linear regression models can be found in Supplemental Data.

Mercury analyses

Mercury concentrations were determined on aliquots with an Advanced Mercury Analyzer spectrophotometer, Altec AMA-254 (aliquots of blood ~2 mg dry wt; feathers ~1 mg dry wt; and muscle ~5 mg dry wt) as described in Bustamante et al. (2006). Measurements were repeated 2 to 3 times for each sample, until the relative standard deviation was <10%. For each set of samples, accuracy and reproducibility of the results were tested by preparing analytical blanks and performing replicate measurements of certified reference materials (TORT-2: lobster hepatopancreas, certified concentration 0.27 ± 0.06 µg g^{-1} dry wt; DOLT-5: dogfish liver, certified concentration 0.44 ± 0.18 µg g^{-1} dry wt; National Research Council of Canada). Measured Hg concentrations for the certified reference materials were 0.26 ± 0.02 µg g^{-1} dry weight ($n = 18$) and 0.38 ± 0.01 µg g^{-1} dry weight ($n = 7$) for TORT-2 and DOLT-5, respectively, corresponding to a recovery rate of $96 \pm 7\%$ for TORT-2 and $100 \pm 2\%$ for DOLT-5. The limit of detection was 0.005 µg g^{-1} dry weight. Mercury concentrations were expressed in µg g^{-1} dry weight.

Determination of blood cell profiles

Blood smears were fixed in methanol (100%) for 30 s, air-dried, stained in a diluted Giemsa solution (ratio of 1:5), rinsed with desalted water, and finally air-dried. The stained blood smears were examined under an optical microscope (Zeiss Axiolab) at a magnification of ×1000 with oil immersion. Heterophils and lymphocytes were counted according to the criteria of Hawkey et al. (1989) until the cumulative total was at least 100 leucocytes. In addition, the number of leucocytes per 10 000 erythrocytes was calculated by counting the number of all erythrocytes every 10th microscopic visual field, and multiplying the mean number of erythrocytes per field by the number of microscopic visual fields that were scanned until 100 leucocytes had been reached for each sample—a method

having a high repeatability according to Lobato et al. (2005). All cell counts were done by a single observer.

Statistical analyses

Statistical analyses were performed using R Ver 3.6.1 (R Development Core Team 2019). Normal distribution of the data and homogeneity of variances were checked using Shapiro–Wilk and Fisher (muscle values) or Bartlett tests (blood and feather values), respectively. Blood and feather Hg concentrations were transformed with $\log_{10}(Hg_{blood})$ and $\log_{10}(Hg_{feathers} + 1)$, respectively, to reduce skewness and heterogeneity before carrying out statistical analyses. According to the results, parametric or nonparametric tests were performed.

Species differences in Hg, $\delta^{13}C$, $\delta^{15}N$, and TP_{LM} were tested using t tests or Mann–Whitney (muscle values), or analysis of variance (ANOVA) or Kruskal–Wallis tests (blood and feather values). Then, post hoc tests were conducted with Tukey multiple comparisons tests or pairwise comparisons using Dunn's test for multiple comparisons of independent samples (correcting p values with the Bonferroni method). Different tissue types assimilate isotopes in a different way (i.e., isotopic routing; Martinez del Rio et al. 2009) hence comparisons were carried out on the same tissue type.

Univariate analyses using Pearson correlation rank tests were conducted to study the relationships between Hg concentrations and continuous explanatory variables ($\delta^{13}C$, $\delta^{15}N$, or TP_{LM}) and between feeding habitat ($\delta^{13}C$) and diet ($\delta^{15}N$), separately for each tissue type. The correlation between $\delta^{13}C$ and TP_{LM} was not investigated because the latter value was calculated using linear regression models including $\delta^{13}C$ values; therefore, these 2 parameters were not independent. The relationship between blood Hg concentrations and heterophil:lymphocyte ratios and between Hg concentrations and the number of leucocytes per 10 000 erythrocytes was also tested with Pearson correlations, separately for each species because the values were species-specific.

Multifactorial analyses were carried out to test the influence of species, foraging habitat ($\delta^{13}C$), and diet ($\delta^{15}N$ and TP_{LM}) on Hg concentrations using generalized linear models. Models were applied separately to blood, feather, and muscle data. Generalized linear models with a normal distribution and an identity-link function were parameterized as follows: Hg concentrations as the response variable; species as a factor; and $\delta^{13}C$, $\delta^{15}N$, and TP_{LM} as continuous covariates. Biologically relevant models were constructed incorporating the different variables and their interactions. Significantly correlated continuous variables ($\delta^{13}C$ and $\delta^{15}N$) were not included in the same models. Also, $\delta^{13}C$ and TP_{LM} were not included in the same models because they were not independent—as was the case for $\delta^{15}N$ and TP_{LM}. Akaike information criterion adjusted for small sample sizes (AIC_C) was used to select the most parsimonious models (Burnham and Anderson 2002). The model with the lowest AIC_C value was considered to be the most accurate. The models with AIC_C values differing by less than 2 are fairly similar in their ability to describe the data, and the model including the least number of parameters was considered as the most accurate according to the principle of parsimony. Akaike weight was calculated to assess the likelihood of the models (Johnson and Omland 2004), and model fit was checked by residual analysis.

Differences were considered significant with $p < 0.05$. Values were mean ± standard deviation.

RESULTS

Hg concentrations and inter-specific comparisons

Blood and feather Hg concentrations varied widely within the Chatham Island seabird community (Table 2), with mean values ranging in blood from $0.40 \pm 0.09\,\mu g\,g^{-1}$ dry weight in broad-billed prions to $11.72 \pm 3.58\,\mu g\,g^{-1}$ dry weight in Magenta petrels, and in feathers from $0.49 \pm 0.23\,\mu g\,g^{-1}$ dry weight in grey-backed storm petrels to $34.14 \pm 6.83\,\mu g\,g^{-1}$ dry weight in Chatham petrels. In blood, the lowest Hg concentration occurred in a broad-billed prion ($0.28\,\mu g\,g^{-1}$ dry wt), and in feathers in a common diving petrel ($0.12\,\mu g\,g^{-1}$ dry wt). The highest blood and feather Hg concentrations were both recorded in Magenta petrels, 16.68 and $43.25\,\mu g\,g^{-1}$ dry weight, respectively. Muscle Hg concentrations ranged from $0.21\,\mu g\,g^{-1}$ dry weight in a broad-billed prion to $0.56\,\mu g\,g^{-1}$ dry weight in a white-faced storm petrel. Mean Hg muscle values were $0.37 \pm 0.09\,\mu g\,g^{-1}$ dry weight in broad-billed prions, and $0.44 \pm 0.10\,\mu g\,g^{-1}$ dry weight in white-faced storm petrels. Interspecific Hg concentration differences were significant both in blood (ANOVA, $F_{6,58} = 160.6$, $p < 0.001$) and in feathers (ANOVA, $F_{6,60} = 241.4$, $p < 0.001$), whereas muscle values were not found to vary significantly between the 2 species investigated (t test, $t = -1.6$, $df = 17.9$, $p = 0.124$; Figure 1).

Stable isotopes

Foraging habitats ($\delta^{13}C$) varied significantly among seabird species (blood, Kruskal–Wallis test, $H = 34.2$, $df = 6$, $p < 0.001$; feathers, Kruskal–Wallis test, $H = 69.2$, $df = 6$, $p < 0.001$; muscle, t test, $t = -3.1$, $df = 17$, $p = 0.006$; Table 2; Figure 2). Trophic positions also showed inter-specific differences, as reflected by $\delta^{15}N$ values (blood, Kruskal–Wallis test, $H = 54.6$, $df = 6$, $p < 0.001$; feathers, Kruskal–Wallis test, $H = 56.8$, $df = 6$, $p < 0.001$; muscle, t test, $t = -5.1$, $df = 16.6$, $p < 0.001$) and TP_{LM} (blood, Kruskal–Wallis test, $H = 58.1$, $df = 6$, $p < 0.001$; feathers, Kruskal–Wallis test, $H = 43.1$, $df = 6$, $p < 0.001$; muscle, Mann–Whitney test, $W = 12$, $p = 0.005$; Table 2; Figure 2).

Relationships between foraging habitat ($\delta^{13}C$) and trophic position ($\delta^{13}C$ or TP_{LM}) show a global trophic resource partitioning among the community—as highlighted by standard ellipse areas (SEA_c) corrected for small sample size (representing trophic niche width; Figure 3). Blood values indicate that common diving petrels and the 2 storm petrel species (grey-backed and white-faced storm petrels) share similar isotopic niches during the incubation and chick-rearing periods,

TABLE 2: $\delta^{13}C$, $\delta^{15}N$, trophic positions inferred from CSIA-AA methods,[a] trophic positions inferred from linear models,[b] Hg concentrations, heterophil:lymphocyte ratios, and number of leucocytes per 10 000 erythrocytes of the 7 Procellariiformes species from the Chatham Islands, New Zealand[c]

Species[d]	Tissue	n	$\delta^{13}C$ (‰)	$\delta^{15}N$ (‰)	TP_{CSIA}	TP_{LM}	Hg ($\mu g\,g^{-1}$ dry wt)	H:L	Leucocytes/10 000 erythrocytes
BBP	Blood	9	−19.08 ± 0.16	8.03 ± 0.58	NA	3.27 ± 0.06	0.40 ± 0.09 (0.28–0.57)	0.89 ± 0.69	36 ± 11
	Feathers	10	−17.57 ± 0.32	13.64 ± 0.82	3.55 ± 0.10	3.90 ± 0.06	1.00 ± 0.39 (0.33–1.53)		
	Muscle	10	−19.70 ± 0.53	8.12 ± 0.88	3.15 ± 0.17	3.37 ± 0.15	0.37 ± 0.09 (0.24–0.53)		
CHPE	Blood	9	−18.47 ± 0.23	14.77 ± 0.98	3.96 ± 0.07	3.99 ± 0.11	4.27 ± 0.93 (2.32–5.22)	0.57 ± 0.43	48 ± 17
	Feathers	10	−15.74 ± 0.38	18.07 ± 1.36	4.18 ± 0.11	4.03 ± 0.10	9.56 ± 2.38 (6.53–13.23)		
CODP	Blood	10	−19.12 ± 0.53	9.35 ± 0.74	3.37 ± 0.23	3.44 ± 0.05	0.94 ± 0.16 (0.78–1.29)	0.93 ± 0.50	34 ± 10
	Feathers	10	−21.37 ± 1.77	8.05 ± 1.19	3.81 ± 0.24	3.90 ± 0.15	0.98 ± 0.55 (0.12–1.71)		
GBSP	Blood	10	−18.98 ± 0.14	9.76 ± 0.45	3.54 ± 0.12	3.47 ± 0.06	0.56 ± 0.16 (0.43–0.84)	1.34 ± 1.02	29 ± 12
	Feathers	10	−17.74 ± 0.21	9.53 ± 0.33	3.82 ± 0.13	3.65 ± 0.03	0.49 ± 0.23 (0.13–0.99)		
MAPE	Blood	7	−18.54 ± 0.61	14.57 ± 1.51	4.06 ± 0.10	3.97 ± 0.16	11.72 ± 3.58 (7.92–16.67)	NA	NA
	Feathers	8	−16.28 ± 0.79	17.30 ± 3.40	4.21 ± 0.10	4.03 ± 0.19	34.14 ± 6.83 (27.34–45.69)		
SOSH	Blood	10	−20.42 ± 1.27	10.32 ± 0.86	3.85 ± 0.13	3.74 ± 0.14	1.13 ± 0.39 (0.63–1.91)	1.52 ± 0.50	61 ± 15
	Feathers	10	−18.56 ± 1.19	12.87 ± 2.23	3.87 ± 0.15	3.95 ± 0.09	2.74 ± 0.80 (1.31–4.42)		
WFSP	Blood	10	−19.14 ± 0.23	9.82 ± 0.39	NA	3.50 ± 0.05	0.93 ± 0.26 (0.52–1.43)	3.77 ± 2.03	84 ± 45
	Feathers	10	−16.55 ± 0.26	12.04 ± 1.58	3.52 ± 0.40	3.70 ± 0.09	1.66 ± 0.51 (1.05–2.61)		
	Muscle	10	−19.03 ± 0.44	9.88 ± 0.65	NA	3.49 ± 0.07	0.44 ± 0.10 (0.21–0.56)		

[a]TP_{CSIA}, $n = 5$ per tissue for each species.
[b]TP_{LM}.
[c]Values are mean ± standard deviation, with ranges in parentheses for Hg concentrations.
[d]See Table 1 for species abbreviations.
$\delta^{13}C$ and $\delta^{15}N$ = stable isotope signatures of carbon and nitrogen; CSIA-AA = compound-specific isotopic analyses of amino acids; TP_{CSIA} = trophic positions inferred from CSIA-AA; TP_{LM} = trophic positions inferred from linear models; H:L ratios = heterophil:lymphocyte ratios; ‰ = parts per thousand; NA = not available.

potentially competing for the same crustacean prey species in the vicinity of the Chatham Islands. However, common diving petrels often dive at 10 m below the water surface (Bocher et al. 2000b; Taylor 2008), whereas storm petrels obtain prey at the sea surface. Broad-billed prions and sooty shearwaters also share similar trophic niches during the inter-breeding season, as indicated by their feather isotopic signatures. Chatham and Magenta petrels share similar trophic niches during both breeding and inter-breeding seasons.

Measures of uncertainty and central tendency of Bayesian standard ellipse areas (SEA_B) in blood and feathers tend to indicate that Magenta petrels and sooty shearwaters are generalist predators during breeding and inter-breeding periods. The other species are more specialized predators all year round, apart from common diving petrels that seem to display a specialized diet while breeding and a more generalist feeding behavior during the inter-breeding season (Figure 4). Moulting common diving petrels may be less proficient at diving as they lose wing feathers, and may be more opportunistic and take prey that is present on the sea surface.

The overall correlation between the foraging habitat ($\delta^{13}C$) and the diet ($\delta^{15}N$) was significant in all tissue types: blood (Pearson's correlation, $r = 0.46$, $P < 0.001$, $n = 69$), feathers (Pearson's correlation, $r = 0.73$, $P < 0.001$, $n = 69$), and muscle (Pearson's correlation, $r = 0.46$, $P = 0.042$, $n = 20$; Table 3). At the species level, this correlation was only found in common diving petrel and sooty shearwater in blood, and in sooty shearwater and white-faced storm petrel in feathers.

Influence of feeding ecology on Hg concentrations

Overall Hg concentrations were significantly and positively correlated with $\delta^{13}C$ values in blood (Pearson's correlation, $r = 0.25$, $t = 2.0$, $P = 0.047$, $n = 65$), feathers (Pearson's
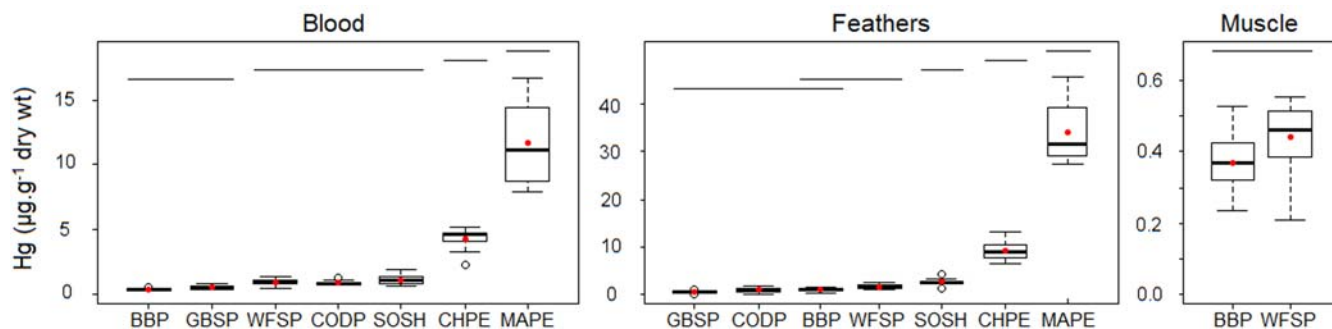
FIGURE 1: Interspecific comparisons of Hg concentrations in blood, feathers, and muscle (see Table 1 for species abbreviations). Quartiles are represented by the upper and lower hinges; maximum and minimum values are the vertical lines; and the median value is the bold line. Red circles represent the mean, whereas black open circles are outliers. Horizontal black lines represent statistically homogeneous groups determined by analysis of variance followed by Tukey honest significant difference test for blood and feathers, and *t* test for muscle.
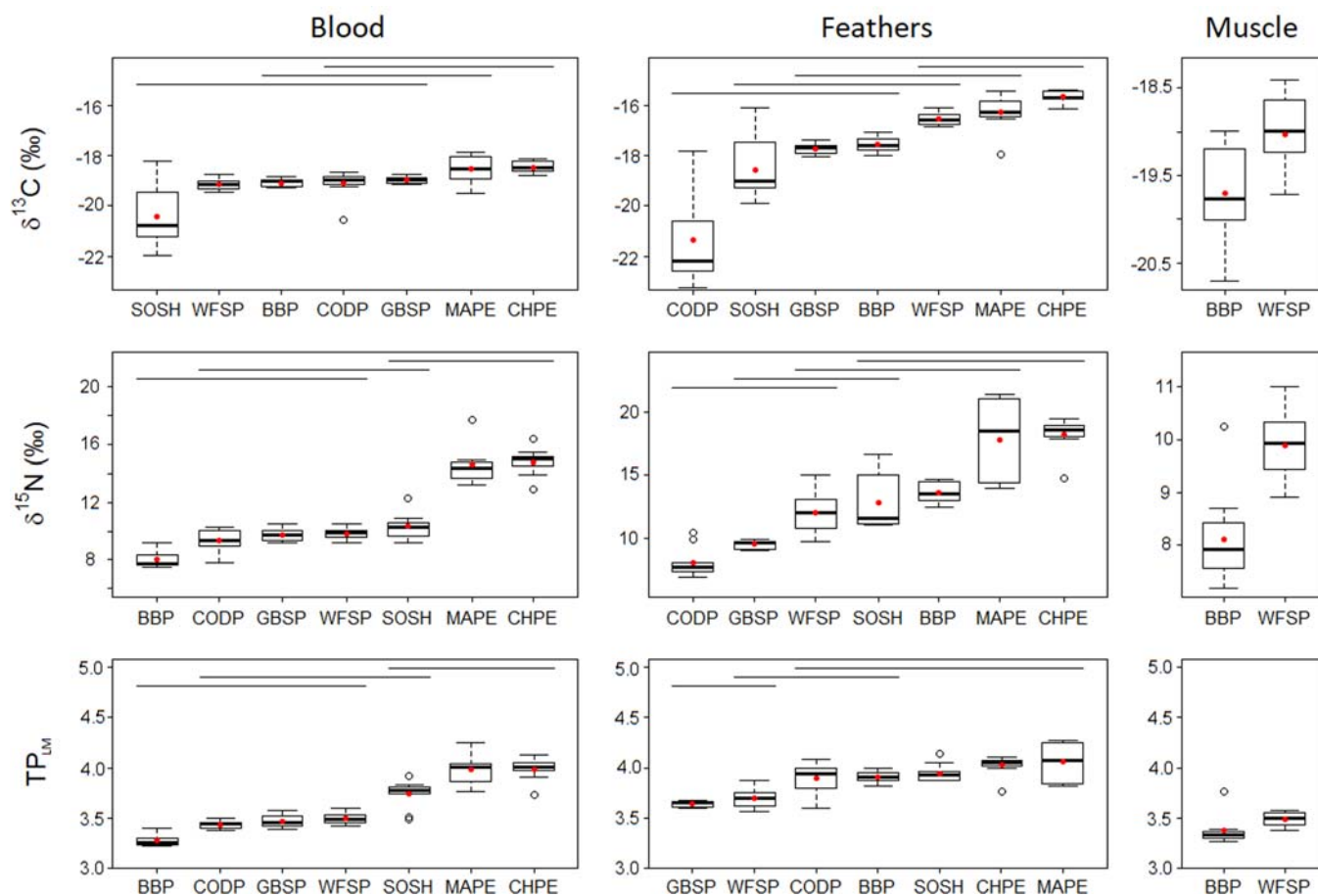
FIGURE 2: Interspecific comparisons of feeding habitats ($\delta^{13}C$) and trophic positions inferred from bulk stable isotopes ($\delta^{15}N$) or derived from compound-specific analyses of amino acids via linear regression models (TP_{LM}) in blood, feathers, and muscle samples (see Table 1 for species abbreviations). Quartiles are represented by upper and lower hinges; vertical lines are maximum and minimum values; and bold line denotes median value. Red circles represent the mean; black open circles are outliers. Horizontal black lines represent statistically homogeneous groups determined by Kruskal-Wallis tests followed by pairwise comparisons using Dunn's test for multiple comparisons of independent samples for blood and feathers, and *t* tests or Mann–Whitney tests for muscle.

correlation, $r = 0.44$, $t = 4.0$, $P < 0.001$, $n = 68$), and muscle (Pearson's correlation, $r = 0.45$, $t = 2.1$, $P = 0.047$, $n = 20$). Mercury values were also significantly and positively correlated with $\delta^{15}N$ values in blood (Pearson's correlation, $r = 0.86$, $t = 13.8$, $P < 0.001$, $n = 65$) and feathers (Pearson correlation, $r = 0.71$, $t = 8.1$, $P < 0.001$, $n = 68$) but not in muscle (Pearson's correlation, $r = 0.29$, $t = 1.3$, $P = 0.215$, $n = 20$). In the same way, Hg concentrations were positively correlated with TP_{LM} in blood (Pearson's correlation, $r = 0.84$, $t = 12.1$, $P < 0.001$, $n = 65$), feathers (Pearson's correlation, $r = 0.55$, $t = 5.3$, $P < 0.001$, $n = 67$) but not in muscle samples (Pearson's correlation, $r = 0.01$, $t = 0.1$, $P = 0.953$, $n = 20$). Relationships between Hg concentrations and feeding habitats ($\delta^{13}C$) or diet ($\delta^{15}N$ or TP_{LM}) in blood, feathers, and muscle are presented in Figures 5 and 6.

In multivariate analyses, the most parsimonious generalized linear models selected by AIC_C values showed that the species and the feeding habitat ($\delta^{13}C$) are the main drivers of Hg concentrations, both in blood and feathers (Table 4). In muscle samples, models including feeding habitat and species were fairly similar in their ability to describe the data, with ΔAIC_C values differing by less than 2 (Table 4) but both had a low likelihood.

Influence of Hg on blood cell profiles

The number of leucocytes per 10 000 erythrocytes and the heterophil:lymphocyte ratio were determined on blood smears of all species except the Magenta petrel (Table 2). No significant correlation was detected between the number of leucocytes per 10 000 erythrocytes and blood Hg values (Pearson's correlations, all $P > 0.05$). Similarly, no significant correlation was found between heterophil:lymphocyte ratios and Hg levels in blood (Pearson's correlations, all $P > 0.05$) except in broad-billed prions (Pearson's correlation, $r = -0.76$, $t = -3.1$, $P = 0.018$, $n = 9$).

DISCUSSION

Mercury concentrations varied considerably among Chatham Islands seabirds, where Hg concentrations in blood were approximately 29 times higher and Hg levels in feathers were approximately 35 times higher in Magenta petrels than in the least contaminated species. We recorded the lowest concentrations of Hg in blood and feathers in seabirds feeding mainly on
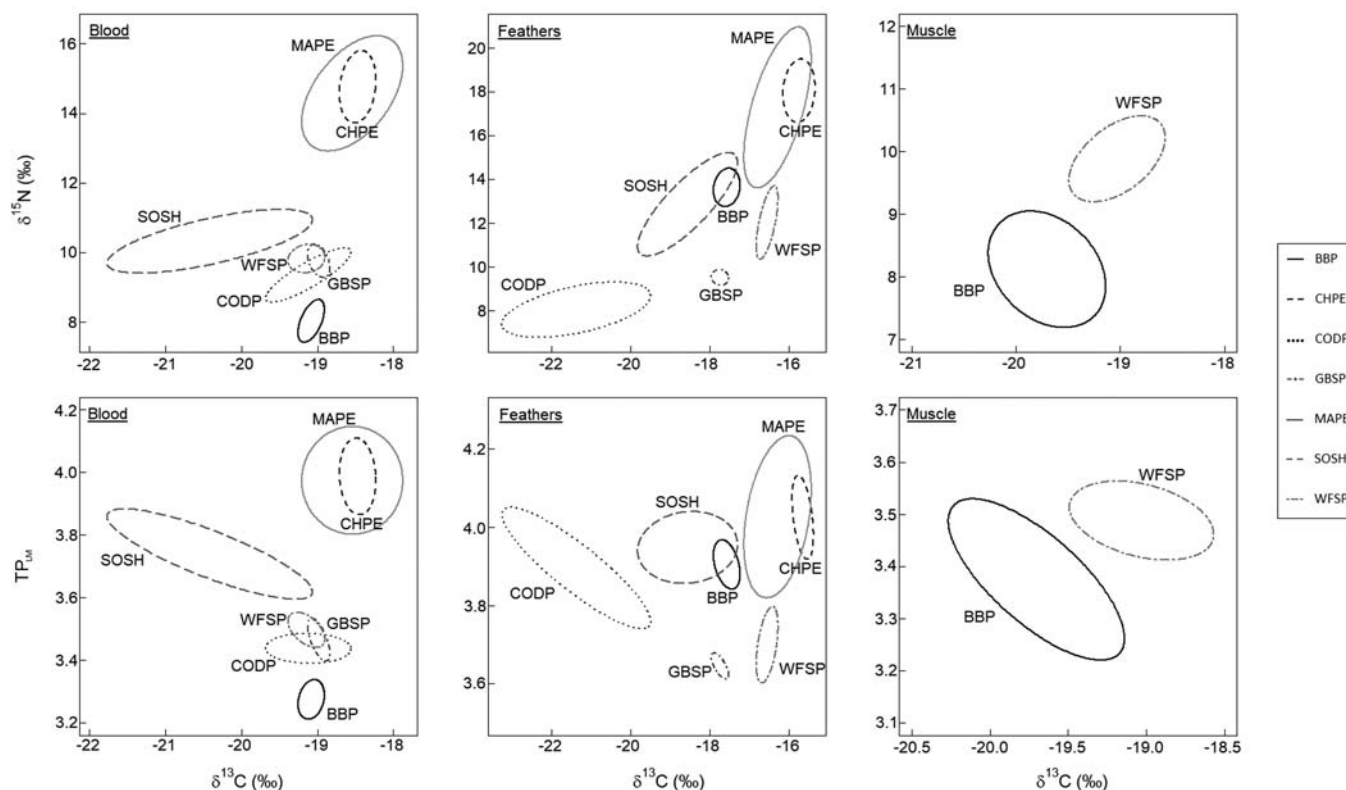
FIGURE 3: Relationships between foraging habitat ($\delta^{13}C$) and trophic position ($\delta^{15}N$ or TP_{LM}) in blood, feathers, and muscle (see Table 1 for species abbreviations). Standard ellipse areas corrected for small sample size were estimated using stable isotope Bayesian ellipses in R (Jackson et al. 2011).
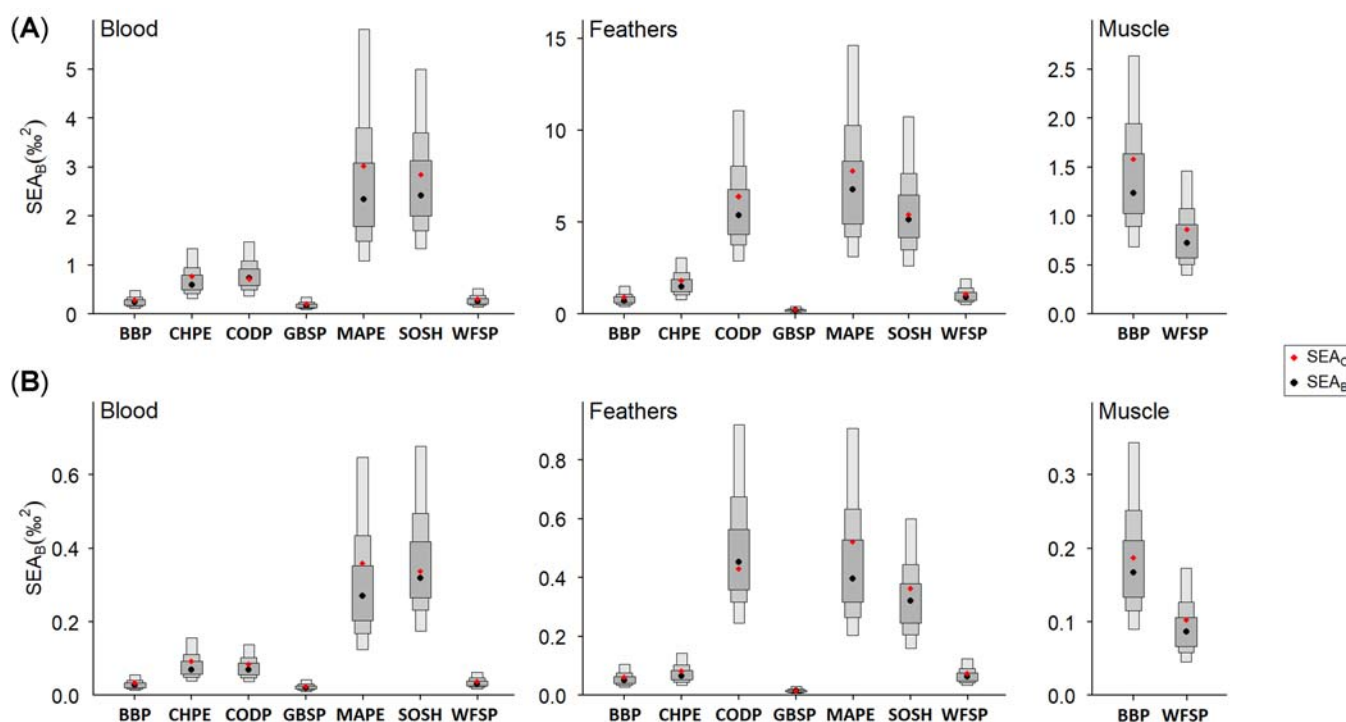
FIGURE 4: Measures of uncertainty and central tendency of Bayesian standard ellipse areas (SEA_B) based on: (**A**) Feeding habitats ($\delta^{13}C$ ‰) and trophic positions inferred from bulk stable isotopes ($\delta^{15}N$ ‰), or (**B**) Feeding habitats ($\delta^{13}C$) and trophic positions derived from compound-specific analyses of amino acids via linear regression models (TP_{LM}) in blood, feathers, and muscle of the 7 seabird species from the Chatham Islands, New Zealand (see Table 1 for species abbreviations). Black dots represent their mode; shaded boxes display 50, 75, and 95% credible intervals from dark to light gray, respectively; red dots identify standard ellipse areas corrected for small sample size (SEA_c) estimates.

TABLE 3: Pearson's correlations between $\delta^{13}C$ and $\delta^{15}N$ in blood, feathers, and muscle of the 7 seabird species from the Chatham Islands[a,b]

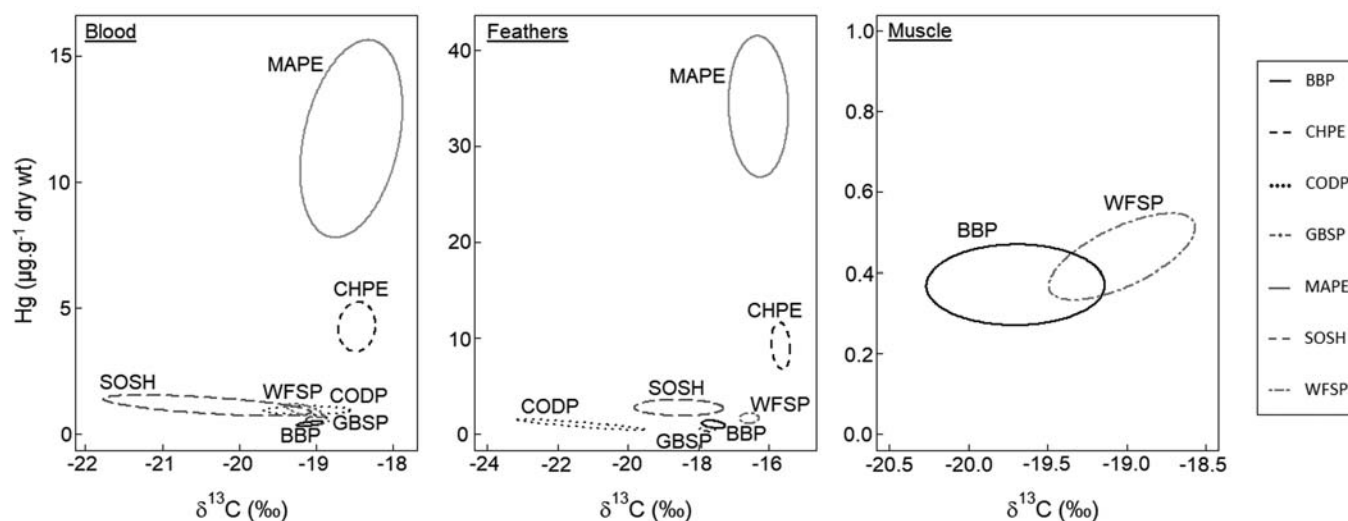| Species	Blood			Feathers			Muscle		
	n	r	p	n	r	p	n	r	p
BBP	9	0.54	0.135	10	0.14	0.702	10	−0.29	0.424
CHPE	9	0.18	0.640	9	0.20	0.597	NA	NA	NA
CODP	10	0.85	*0.002*	10	0.51	0.129	NA	NA	NA
GBSP	10	−0.40	0.250	10	−0.11	0.768	NA	NA	NA
MAPE	11	0.42	0.196	10	0.58	0.080	NA	NA	NA
SOSH	10	0.68	*0.030*	10	0.82	*0.004*	NA	NA	NA
WFSP	10	0.12	0.736	10	0.66	*0.039*	10	0.49	0.146
Overall	69	0.46	*<0.001*	69	0.73	*<0.001*	20	0.46	*0.042*

[a]Significant correlations appear in *italics*.
[b]See Table 1 for species abbreviations.
$\delta^{13}C$ and $\delta^{15}N$ = stable isotope signatures of carbon and nitrogen; NA = not available.

crustaceans—broad-billed prions, common diving petrels, grey-backed storm petrels, and white-faced storm petrels. Sooty shearwaters that feed both in neritic and oceanic waters all year-round and on a broader prey spectrum had intermediate Hg levels. The highest Hg concentrations in blood and feathers were recorded in the 2 gadfly petrels or *Pterodroma* species, namely Magenta and Chatham petrels, which are oceanic foragers with a cephalopod- and fish-based diet (Table 1). Variation displayed in Hg concentrations in blood and feathers among the Chatham Island seabirds can be explained by the different feeding habits and locations of the different species. Muscle samples could be opportunistically obtained in only 2 of the 7 species investigated. Mercury concentrations in muscle were relatively low and were correlated with feeding habitat but not with diet. Multivariate analyses failed to explain the variations in muscle Hg concentrations by differences in feeding ecology or species' affiliations.

Muscle is considered as a temporary storage tissue for Hg that is subsequently excreted in the feathers during the moult (Lewis and Furness 1991). Indeed, the plumage is the main route for Hg elimination (Monteiro and Furness 1995; Albert et al. 2019). However, feather Hg represents the exposure since the previous moult, whereas stable isotope values reflect the diet at the time of feather synthesis; thus, there is a mismatch between both parameters (Bond 2010). Apart from the breeding period, seabirds are no longer restricted to the vicinity of the breeding colony and several species present a very large foraging range. Hence, it is difficult to properly determine a specific foraging area for migrating birds and caution is required when trying to interpret dietary Hg exposure using stable isotopes as a proxy in adult feathers (Bond 2010; Carravieri et al. 2013). In contrast, stable isotopes in blood provide information about the foraging ecology 1 to 2 mo before sampling (Bearhop et al. 2002; Vander Zanden et al. 2015), which is approximately the biological half-life of Hg in this tissue type (Monteiro and Furness 2001).

The high Hg concentrations detected in blood and feathers of Magenta and Chatham petrels potentially put these 2 threatened species at risk of suffering detrimental effects from Hg exposure (Eisler 1987; Burger and Gochfeld 1997; Evers

FIGURE 5: Relationships between Hg concentrations in blood, feathers, and muscle and trophic habitat ($\delta^{13}C$) of seabirds breeding in the Chatham Islands, New Zealand (see Table 1 for species abbreviations). Standard ellipse areas corrected for small sample size were estimated using stable isotope Bayesian ellipses in R (Jackson et al. 2011).
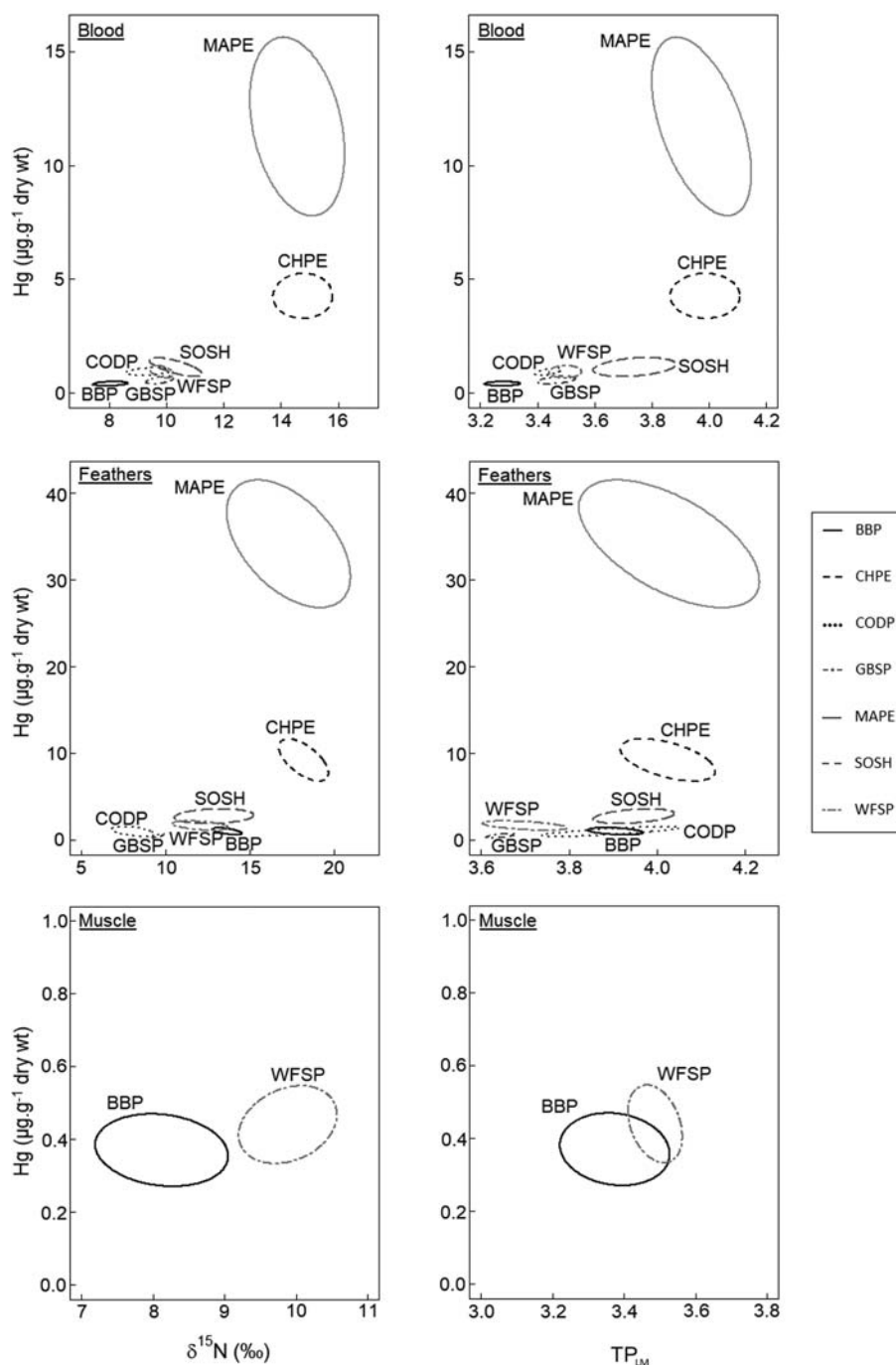
FIGURE 6: Relationships between Hg concentrations and trophic positions inferred from bulk stable isotope analyses ($\delta^{15}N$ ‰) or derived from compound-specific analyses of amino acids via linear regression models (TP$_{LM}$) in blood, feathers, and muscle (see Table 1 for species abbreviations). Standard ellipse areas corrected for small sample size were estimated using stable isotope Bayesian ellipses in R (Jackson et al. 2011).

et al. 2008; Tartu et al. 2013; Costantini et al. 2014; Goutte et al. 2014; Tartu et al. 2015; Ackerman et al. 2016).

Influence of trophic position on Hg concentrations

Mercury concentrations in blood and feathers were significantly and positively correlated with trophic levels, attesting to the occurrence of efficient Hg biomagnification processes

within the food web. The 2 different methods used in the present study to infer trophic levels (raw $\delta^{15}N$ and TP$_{LM}$) noticeably led to similar conclusions regarding the diet of the birds and its influence on Hg concentrations.

Blood and feather stable isotope analyses revealed that Chatham and Magenta petrels share the same isotopic niche and therefore potentially the same trophic niche, with Magenta petrels having a larger isotopic niche than Chatham petrels. Both species had the highest trophic positions among the species breeding in the Chatham Islands, which confirms their

TABLE 4: Akaike information criterion corrected for small sample size model ranking constructed incorporating the different variables and their interactions for blood, feather, and muscle Hg concentrations within the Chatham Islands' avian community.[a,b,c,d]

Models	Number of parameters	AIC$_C$	ΔAIC$_C$	w_i
BLOOD ($n = 65$)				
Species + δ^{13}C	9	–87.6	0.0	0.58
FEATHERS ($n = 67$)				
Species + δ^{13}C	9	–129.5	0.0	0.90
MUSCLE ($n = 20$)				
δ^{13}C	3	–32.8	0.0	0.35
Null	2	–31.1	1.7	0.15
Species	3	–31.0	1.8	0.14

[a]Models are GLMs with a normal distribution and an identity link function.
[b]Model with ΔAIC$_C$ = 0.00 is considered the best fit to the data.
[c]Models differing by <2 are fairly similar in their ability to describe the data.
[d]Only models with ΔAIC$_C$ < 2 are shown in this table.
AIC$_C$ = Akaike information criterion corrected for small sample size; ΔAIC$_C$ = scaled AIC$_C$; w_i = Akaike weight (likelihood of the model, with sum for all models Σw_i = 1.00, see Johnson and Omland 2004); GLMs = generalized linear models; δ^{13}C = stable isotope signature of carbon.

fish- and cephalopod-based diet. Nevertheless, Magenta petrels interestingly had much higher blood and feather Hg concentrations than Chatham petrels. Despite their similar trophic positions, Chatham and Magenta petrels seem to target distinct prey species. Chatham petrels are likely to forage on juvenile squids, nocturnally rising myctophids, and small zooplankton, mainly at night during the moult and both day and night during breeding (G. Taylor, unpublished data). Magenta petrels can cut up larger squids floating dead on the surface and forage on squid and fish both day and night throughout the year (G. Taylor, unpublished data). Indeed, the consumption of some specific prey types (e.g., mesopelagic fishes and large cephalopods) seems to be a more important factor in explaining Hg exposure than trophic position (Thompson et al. 1998; Blévin et al. 2013). In addition, Chatham petrel has a length of 30 cm and a weight of 200 g on average, whereas Magenta petrel is slightly bigger, with a length of 38 cm and a weight of 475 g (Heather and Robertson 2005). This size difference allows Magenta petrels to feed on larger prey than Chatham petrels, and can partly explain the variation in Hg levels recorded between these 2 species because Hg body burdens are highly and positively correlated to size and age in fishes (Kojadinovic et al. 2006).

Influence of feeding habitats on Hg concentrations

Blood Hg concentrations and foraging habitats of Chatham Island seabirds during the breeding season are in good agreement with our hypothesis that oceanic seabirds feeding on mesopelagic prey are more Hg-contaminated than birds relying on epipelagic prey caught in neritic waters (Monteiro et al. 1996; Ochoa-Acuña et al. 2002; Carravieri et al. 2014a).

At-sea tracking of breeding sooty shearwaters revealed their ability to alternate short provisioning trips (1–3 d) in the vicinity of the colony and longer trips (5–15 d) along the Antarctic Polar Front, which reduces competition close to the breeding grounds and allows vast colonies to persist (Weimerskirch 1998; Shaffer et al. 2009). A broad range of δ^{13}C blood values was found for this species, which can be related to the latitudinal gradient in δ^{13}C values between subtropical and Antarctic waters (Cherel and Hobson 2007; Jaeger et al. 2010). Our findings are in good agreement with the δ^{13}C isoscapes already available in the literature for the Southern Indian Ocean. Except for sooty shearwaters, seabird species breeding in the Chatham Islands had blood δ^{13}C signatures typical of the subtropical zone.

Taking into account the latitudinal δ^{13}C isoscapes available for marine predators in the Southern Ocean (Cherel and Hobson 2007; Jaeger et al. 2010), the positive correlation between Hg concentrations and δ^{13}C values tends to confirm that species foraging in cold sub-Antarctic waters were less prone to contamination than species foraging in warmer subtropical waters. Despite the poleward increase in surface waters Hg concentrations (Cossa et al. 2011), previous investigations considering a larger latitudinal range from the Antarctic to the subtropics found the same contamination pattern (Blévin et al. 2013; Carravieri et al. 2017, 2020b), which was attributed to the higher complexity of food webs at lower latitudes (Carravieri et al. 2014b).

Previous investigations using geolocation-immersion loggers have shown that, during breeding, Chatham petrels forage between the subtropical convergence and the sub-Antarctic front during the pre-laying exodus and the incubation period. They are restricted to the Bollons Seamount south of the Chatham Islands during the chick-rearing period. During the non-breeding period, they migrate to the eastern South Pacific Ocean, to the outer edge of the Humboldt Current system adjacent to Peru and Chile (Rayner et al. 2012), a region renowned for its high biological productivity and characterized by complex food webs. Magenta petrels forage south and east of the Chatham Islands during the breeding season (Imber et al. 1994) and disperse widely during the inter-breeding period across the Pacific Ocean from the Tasman Sea to the South American west coast, foraging at relatively low latitudes (Giglioli and Salvadori 1869; Taylor 2013; G. Taylor, unpublished data).

The New Zealand region and the Pacific Ocean are characterized by numerous geothermal features, natural sources of Hg emission (Weissberg and Zobel 1973; Weissberg and Rohde 1978; Chrystall and Rumsby 2009). Seabirds in New Zealand are therefore potentially exposed to higher Hg levels during the breeding season in comparison with birds breeding at sites with a lower geothermal activity. The very high Hg concentrations detected in *Pterodroma* species breeding in New Zealand could partly result from the substantial geothermal Hg emissions in this region. Research addressing the Hg contamination in chicks rather than in adults is recommended to better investigate the Hg bioavailability to top predators in the New Zealand region (Blévin et al. 2013; Carravieri et al. 2016).

The eastern boundary Humboldt Current is responsible for the transport of cold, low-salinity, and nutrient-rich waters from high to low latitudes off the western coast of South America

466

Environmental Toxicology and Chemistry, 2021;40:454–472—J. Thébault et al.

(Acha et al. 2004). The upwelling ecosystems in this region are recognized as the most productive systems of the World Ocean. They support a remarkably high primary production that is decomposed in the water column—a process requiring the consumption of dissolved oxygen. The high oxygen demand participates in the production of a subsurface and mid-water oxygen minimum zone (<20 µmol kg^{-1}) in the continental margins off Peru and northern Chile (Cline and Richards 1972; Codispoti and Christensen 1985; Minami and Ogi 1997; Fuenzalida et al. 2009). In this type of naturally hypoxic environment, the methylation of Hg by anaerobic microorganisms (Hsu-Kim et al. 2013) could be enhanced, making Hg highly bioavailable for marine organisms (Stewart et al. 1999). A recent investigation of Hg speciation and distribution across the eastern South Pacific Ocean revealed the enrichment in total Hg in the Peru upwelling region, with monoMeHg accounting for up to 20% of the upwelling flux. Methylated Hg concentrations were greatest in the suboxic oxygen minimum zone underlying productive surface waters (Bowman et al. 2016). A high Hg bioavailability in the Humboldt Current system region could partly explain the high Hg concentrations recorded in Magenta and Chatham petrels. However, an earlier study comparing the trophic characteristics of ecosystems in explaining the differences in Hg bioaccumulation and biomagnification among food webs and systems found that organisms from oligotrophic waters—with a low primary production—tend to bioaccumulate more Hg than organisms from highly productive ecosystems (Chouvelon et al. 2018). The high productivity of the Humboldt Current system is likely to result in a dilution of Hg in the system and would limit marine predator's exposure. Very few data are available regarding the Hg exposure of seabirds foraging in the Humboldt Current region (Gochfeld 1980; Álvarez-Varas et al. 2018). Relatively low Hg breast feather levels between 0.5 and 2.0 µg g^{-1} dry weight were found in piscivorous species sampled on the Peruvian coast (Gochfeld 1980). However, upwelling regions are predicted to grow in size and intensity during this century (Capone and Hutchins 2013), potentially increasing the flux of Hg near the coasts of Peru and Chile (Bowman et al. 2016). The high marine productivity in the eastern South Pacific Ocean sustains many populations of seabird species and has allowed the development of some of the world's largest fisheries (Swartz et al. 2010). Thus, monitoring the degree of Hg bioavailability in this area is of concern, both for biodiversity conservation and public health issues.

Comparison with other breeding sites and seabird species

For most of the species investigated in the present study, only feather Hg concentrations were reported previously in the literature. To the best of our knowledge, the present study is the first to report blood and muscle Hg concentrations for these Procellariiformes, as well as feather Hg concentrations in Chatham and Magenta petrels. At the species level, feather Hg concentrations of Chatham Islands seabirds globally fall within the concentration range already documented at other breeding sites from the subtropical to the Antarctic zones (Table 5; Ochoa-Acuña et al. 2002; Anderson et al. 2009; Carravieri et al. 2014a, 2014b, 2014c; Becker et al. 2002, 2016; Lyver et al. 2017). These results suggest that these species may forage in marine habitats of similar Hg bioavailability during the inter-breeding period when they moult at sea, and moderate Hg variations observed may arise from inter-site dietary differences.

Muscle Hg concentrations in zooplankton-eating species from the Kerguelen Islands in the southern Indian Ocean were similar to those found in broad-billed prions and white-faced storm petrels breeding in the Chatham Islands. The Kerguelen Islands species were thin-billed prion (*Pachyptila belcheri*: 0.26 ± 0.19 µg g^{-1} dry wt, n = 5), Antarctic prion (*Pachyptila desolata*: 0.08 ± 0.00 µg g^{-1} dry wt, n = 2; 0.28 ± 0.06 µg g^{-1} dry wt, n = 10), South Georgian diving petrel (*Pelecanoides georgicus*: 0.17 ± 0.13 µg g^{-1} dry wt, n = 5), and common diving petrel (*P. urinatrix*: 0.20 ± 0.13 µg g^{-1} dry wt, n = 13; Bocher et al. 2003; Fromant et al. 2016). Species with a broader prey spectrum feeding on both fish and krill such as blue petrel (*Halobaena caerulea*) and white-chinned petrel (*Procellaria aequinoctialis*) had slightly higher muscle Hg concentrations: 1.76 ± 0.91 µg g^{-1} dry weight, n = 10 and 2.86 ± 0.80 µg g^{-1} dry weight, n = 32, respectively (Bocher et al. 2003; Cipro et al. 2014).

Blood and feather Hg concentrations in the Chatham and Magenta petrels are among the highest ever recorded in seabirds around the world (Cherel et al. 2018). Feather Hg concentrations vary widely among *Pterodroma* species, from 0.96 ± 0.31 µg g^{-1} dry weight in Barau's petrel (*P. baraui*) breeding at Réunion Island in the Indian Ocean (Kojadinovic et al. 2007) to 36.48 ± 9.59 µg g^{-1} dry weight in grey-faced petrels breeding in northern New Zealand (Lyver et al. 2017; Table 6). Despite this high variation among species, gadfly petrels consistently rank among the most Hg-contaminated species in all the different environments where they have been studied (Carravieri et al. 2014a). However, the available dataset for the genus *Pterodroma* (reviewed in Table 6) remains largely incomplete because many species have not been sampled, and for several species sample sizes are relatively low (n < 5). Most gadfly petrels are top predators with a cephalopod- or fish-based diet and are therefore prone to bioaccumulating high concentrations of Hg. Their high trophic position may be the major factor explaining their consistent high Hg concentrations but phylogeny could also influence Hg concentrations. Even though the main route for Hg contamination in seabirds is via food intake (Atwell et al. 1998; Burger and Gochfeld 2004), the mechanism underlying bioaccumulation remains poorly understood. Several factors can lead to variation in Hg burdens: phylogeny (physiology and detoxification capabilities; Bearhop et al. 2000a; Cherel et al. 2018), tissue type, and life history traits (nutritional condition, age, and breeding status; Ramos et al. 2013; Carravieri et al. 2014b). *Pterodroma* species are characterized by the presence of helicoidal upper intestines unlike most seabird species with intestines formed of a simple tube (Imber 1985). *Pterodroma* species specialize in foraging over

TABLE 5: Synthesis of Hg concentrations[a] recorded in feathers of adult seabird species investigated in the Chatham Islands and other breeding sites

Common name	Location	Year	Hg	n	References
Broad-billed prion	Chatham Islands	2015	1.00 ± 0.39	10	Present study
	Gough Island	2009	0.75 ± 0.62	10	Becker et al. 2016
Common diving petrel	Chatham Islands	2015	0.98 ± 0.55	10	Present study
	Gough Island	2009	0.58 ± 0.19	10	Becker et al. 2016
	Kerguelen Islands	2003–2011	1.06 ± 0.54	29	Carravieri et al. 2014a, 2014b, 2014c
	Northern New Zealand	2011–2013	3.36 ± 2.02	30	Lyver et al. 2017
	South Georgia	1998	0.59 ± 0.15	2	Becker et al. 2002
	South Georgia	2001–2002	2.90 ± 1.63	15	Anderson et al. 2009
Grey-backed storm petrel	Chatham Islands	2015	0.49 ± 0.23	10	Present study
	Gough Island	2009	1.98 ± 2.07	2	Becker et al. 2016
	Kerguelen Islands	2003–2011	0.51 ± 0.44	23	Carravieri et al. 2014a, 2014b, 2014c
	Marion Island	2011	0.54	1	Becker et al. 2016
Sooty shearwater	Chatham Islands	2015	2.74 ± 0.80	10	Present study
	Chilean coast	1995	1.30 ± 0.20	2 females	Ochoa-Acuña et al. 2002
	Chilean coast	1995	1.90 ± 0.30	6 males	Ochoa-Acuña et al. 2002
White-faced storm petrel	Chatham Islands	2015	1.66 ± 0.51	10	Present study
	Gough Island	2009	1.41 ± 0.44	10	Becker et al. 2016

[a]Mean ± standard deviation; $\mu g\,g^{-1}$ dry weight.

deep ocean basins in lower productivity zones where they exploit scarce and unpredictable oceanic resources at great distances from the colony (Rayner et al. 2012; Taylor et al. 2020). The remarkable coiled structure of their intestines presumably allows the birds to grind out every drop of nutrients from the scattered prey that they feed on. A potential enhanced assimilation efficiency of Hg through helicoidal intestines in comparison with tube-like intestines could partly explain the consistently high concentrations recorded in these species. Approximately 70% of gadfly petrel species are listed as endangered species in the International Union for Conservation of Nature Red List; however, little is known about the ecology of most species and the anthropogenic pressures they may face. Further research addressing their exposure to Hg and other environmental contaminants is required to determine whether these contaminants could contribute to the decline of their populations through long-term effects on reproduction.

Potential adverse effects

Interpreting the impact of observed contaminant concentrations on wild organisms to establish threshold values can be challenging, especially because these animals are potentially exposed to diverse stress factors in their environment or to a cocktail of pollutants (e.g., Goutte et al. 2014). Sensitivity to contaminants varies among species, sex, and age class (Burger and Gochfeld 2004; Heinz et al. 2009; Tartu et al. 2015), and few data are available on Hg threshold values inducing detrimental effects on birds (Eisler 1987; Evers et al. 2008; Goutte et al. 2015; Tartu et al. 2015). Seabirds nevertheless present efficient detoxification processes and therefore may be able to cope with higher Hg exposure than terrestrial birds (Scheuhammer 1987; Carravieri et al. 2017).

Exposure to elevated Hg concentrations has been associated with developmental, behavioral, and physiological impairments in seabirds (Eisler 1987; Burger and Gochfeld 1997; Evers et al. 2008; Tartu et al. 2013, 2015). Laboratory and field studies indicate that concentrations higher than $5\,\mu g\,g^{-1}$ dry weight in feathers can affect reproduction because they are associated with increased hatching failure and sterility in various species (Eisler 1987). In blood, a threshold Hg concentration of $1\,\mu g\,g^{-1}$ wet weight (~$4\,\mu g\,g^{-1}$ dry wt) has been proposed by Ackerman et al. (2016), based on a review of the literature.

Chatham and Magenta petrels breeding in the Chatham Islands showed Hg concentrations exceeding the threshold values and are therefore at risk to suffer detrimental effects from Hg exposure. However, we found no evidence that Hg exposure of Chatham Island seabirds affected their immune system. Unfortunately, no blood smears were available for the Magenta petrel, the species exhibiting the highest Hg concentrations. Even in low concentrations, Hg is known to be immunotoxic in experimental birds (Spalding et al. 2000). Either the heterophil:lymphocyte ratio counting is an ineffective method in demonstrating immunomodulation induced by Hg or the concentrations to which the seabirds are naturally exposed are below threshold effect levels. Nevertheless, the particularly elevated Hg concentrations recorded in Magenta petrels are of concern, given the rarity of the species and its classification as critically endangered (80–100 mature individuals; Taylor et al. 2012) because it may affect other functions such as reproduction. Research addressing the potential Hg impacts on physiology and breeding behavior of adult Magenta petrels and on hatching and fledging success of their chicks is strongly recommended while considering long-term population management. More research on Hg concentrations in other New Zealand species of *Pterodroma* petrels is also recommended because the 2 species with the highest reported Hg concentrations (grey-faced petrels and Magenta petrels; Table 6) occur in this region.

TABLE 6: Synthesis of Hg concentrations[a] recorded in feathers of chicks and adults of *Pterodroma* species from different breeding sites

Species	Location	Year	Chicks	Adults	References
Atlantic petrel (*Pterodroma incerta*)	Gough Island	1983	–	13.90 ± 3.60 (n = 23)	Thompson et al. 1990
	Gough Island	1985	–	13.53 ± 4.14 (3.92–20.09; n = 15)	Thompson et al. 1993
Barau's petrel (*Pterodroma baraui*)	Reunion Island	2001–2004	0.30 ± 0.07 (n = 32)	0.96 ± 0.31 (n = 20)	Kojadinovic et al. 2007
Bonin petrel (*Pterodroma hypoleuca*)	Hawaiian Islands	NA	3.87 ± 0.31 (n = 20)	19.70 ± 1.10 (n = 27)	Gochfeld et al. 1999
Chatham petrel (*Pterodroma axillaris*)	Chatham Islands	2015	–	9.56 ± 2.38 (6.53–13.23; n = 10)	Present study
Cook's petrel (*Pterodroma cooki*)	NA	Before 1992	–	12.40 (n = 1)	Lock et al. 1992
Great-winged petrel (*Pterodroma macroptera*)	Kerguelen Islands	2005	1.64 ± 0.48 (0.96–2.68; n = 10)	15.82 ± 4.44 (9.76–27.13; n = 14)	Blévin et al. 2013, Carravieri et al. 2014a
Grey-faced petrel (*Pterodroma gouldi*)	Marion Island	2011	–	28.04 ± 9.98 (n = 5)	Becker et al. 2016
	New Zealand	2011–2013	–	36.48 ± 9.59 (n = 32)	Lyver et al. 2017
Juan Fernandez's petrel (*Pterodroma externa*)	Chilean coast	1995	–	3.90 ± 0.20 (n = 11 males)	Ochoa-Acuña et al. 2002
Kermadec petrel (*Pterodroma neglecta*)	Chilean coast	1995	–	4.20 ± 0.30 (n = 5 females)	Ochoa-Acuña et al. 2002
Magenta petrel (*Pterodroma magentae*)	Chatham Islands	1995	–	12.00 (n = 2)	Ochoa-Acuña et al. 2002
Soft-plumaged petrel (*Pterodroma mollis*)	Gough Island	2015	–	34.14 ± 6.83 (27.34–45.69; n = 8)	Present study
	Gough Island	1985	–	9.82 ± 2.32 (5.36–13.40; n = 17)	Thompson et al. 1993
	Gough Island	1983	–	10.30 ± 2.30 (n = 21)	Thompson et al. 1990
	Kerguelen Islands	2009	–	15.06 ± 3.51 (9.18–19.98; n = 10)	Becker et al. 2016
	Marion Island	2010–2011	–	12.21 ± 4.23 (4.67–25.48; n = 19)	Carravieri et al. 2014a
	Marion Island	2011	–	7.20 ± 4.98 (1.72–11.55; n = 5)	Becker et al. 2016
Stejneger's petrel (*Pterodroma longirostris*)	Chilean coast	1995	–	7.30 ± 0.80 (n = 2)	Ochoa-Acuña et al. 2002
White-headed petrel (*Pterodroma lessonii*)	Sub-Antarctic Islands	Before 1992	–	24.40 (n = 1)	Lock et al. 1992
	Kerguelen Islands	2002–2003	1.54 ± 0.34 (1.07–1.99; n = 10)	12.43 ± 2.01 (9.22–17.06; n = 10)	Carravieri et al. 2014a

[a]Mean ± standard deviation; µg g^{-1} dry weight.
NA = not available.

REFERENCES

Acha EM, Mianzan HW, Guerrero RA, Favero M, Bava J. 2004. Marine fronts at the continental shelves of austral South America—Physical and ecological processes. *J Mar Syst* 44:83–105.

Ackerman JT, Eagles-Smith CA, Herzog MP, Hartman CA, Peterson SH, Evers DC, Jackson AK, Elliott JE, Vander Pol SS, Bryan CE. 2016. Avian mercury exposure and toxicological risk across western North America: A synthesis. *Sci Total Environ* 568:749–769.

Albert C, Renedo M, Bustamante P, Fort J. 2019. Using blood and feathers to investigate large-scale Hg contamination in arctic seabirds: A review. *Environ Res* 177C:108588.

Álvarez-Varas R, Morales-Moraga D, González-Acuña D, Klarian SA, Vianna JA. 2018. Mercury exposure in Humboldt (*Spheniscus humboldti*) and Chinstrap (*Pygoscelis antarcticus*) penguins throughout the Chilean coast and Antarctica. *Arch Environ Contam Toxicol* 75:75–86.

Anderson ORJ, Phillips RA, McDonald RA, Shore RF, McGill RAR, Bearhop S. 2009. Influence of trophic position and foraging range on mercury levels within a seabird community. *Mar Ecol Prog Ser* 375: 277–288.

Atwell L, Hobson KA, Welch HE. 1998. Biomagnification and bioaccumulation of mercury in an Arctic marine food web: Insights from stable nitrogen isotope analysis. *Can J Fish Aquat Sci* 55:1114–1121.

Bearhop S, Phillips RA, Thompson DR, Waldron S, Furness RW. 2000a. Variability in mercury concentrations of great skuas *Catharacta skua*: The influence of colony, diet and trophic status inferred from stable isotope signatures. *Mar Ecol Prog Ser* 195:261–268.

Bearhop S, Teece MA, Waldron S, Furness RW. 2000b. Influence of lipid and uric acid on δ^{13}C and δ^{15}N values of avian blood: Implications for trophic studies. *Auk* 117:504–507.

Bearhop S, Waldron S, Votier SC, Furness RW. 2002. Factors that influence assimilation rates and fractionation of nitrogen and carbon stable isotopes in avian blood and feathers. *Physiol Biochem Zool* 75:451–458.

Becker PH, González-Solís J, Behrends B, Croxall J. 2002. Feather mercury levels in seabirds at South Georgia: Influence of trophic position, sex and age. *Mar Ecol Prog Ser* 243:261–269.

Becker PH, Goutner V, Ryan PG, González-Solís J. 2016. Feather mercury concentrations in Southern Ocean seabirds: Variation by species, site and time. *Environ Pollut* 216:253–263.

BirdLife International. 2018a. *Pterodroma axillaris*. The IUCN Red List of threatened species 2018: e.T22697949A132613763. [cited 2020 July 2]. Available from: https://www.iucnredlist.org/species/22697949/132613763

BirdLife International. 2018b. *Pterodroma magentae*. The IUCN Red List of threatened species 2018: e.T22698049A131879320. [cited 2020 July 2]. Available from: https://www.iucnredlist.org/species/22698049/131879320

Blévin P, Carravieri A, Jaeger A, Chastel O, Bustamante P, Cherel Y. 2013. Wide range of mercury contamination of Southern Ocean seabirds. *PLoS One* 8:e54508.

Blum JB, Popp BN, Drazen JC, Choy CA, Johnson MW. 2013. Methylmercury production below the mixed layer in the North Pacific Ocean. *Nat Geosci* 6:879–884.

Bocher P, Caurant F, Miramand P, Cherel Y, Bustamante P. 2003. Influence of the diet on the bioaccumulation of heavy metals in zooplankton-eating petrels at Kerguelen archipelago, Southern Indian Ocean. *Polar Biol* 26:759–767.

Bocher P, Cherel Y, Hobson KA. 2000a. Complete trophic segregation between South Georgian and common diving petrels during breeding at Iles Kerguelen. *Mar Ecol Prog Ser* 208:249–264.

Bocher P, Cherel Y, Labat J-P, Mayzaud P, Razouls S, Jouventin P. 2001. Amphipod-based food web: *Themisto gaudichaudii* caught in nets and by seabirds in Kerguelen waters, southern Indian Ocean. *Mar Ecol Prog Ser* 223:261–276.

Bocher P, Labidoire B, Cherel Y. 2000b. Maximum dive depths of common diving petrels (*Pelecanoides urinatrix*) during the annual cycle at Mayes Island, Kerguelen. *J Zool* 251:517–524.

Bond AL. 2010. Relationships between stable isotopes and metal contaminants in feathers are spurious and biologically uninformative. *Environ Pollut* 158:1182–1184.

Bond AL, Diamond AW. 2009. Total and methyl mercury concentrations in seabird feathers and eggs. *Arch Environ Contam Toxicol* 56:286–291.

Bowman KL, Hammerschmidt CR, Lamborg CH, Swarr GJ, Agather AM. 2016. Distribution of mercury species across a zonal section of the eastern tropical South Pacific Ocean (U.S. GEOTRACES GP16). *Mar Chem* 186:156–166.

Brasso RL, Polito MJ. 2013. Trophic calculations reveal the mechanism of population-level variation in mercury concentrations between marine ecosystems: Case studies of two polar seabirds. *Mar Pollut Bull* 75:244–249.

Braune BM, Gaskin DE. 1987. Mercury levels in Bonaparte's gulls (*Larus philadelphia*) during autumn molt in the Quoddy region, New Brunswick, Canada. *Arch Environ Contam Toxicol* 16:539–549.

Burger J. 1993. Metals in avian feathers: Bioindicators of environmental pollution. *Rev Environ Contam Toxicol* 5:203–311.

Burger J, Gochfeld M. 1997. Risk, mercury levels, and birds: Relating adverse laboratory effects to field biomonitoring. *Environ Res* 75:160–172.

Burger J, Gochfeld M. 2004. Marine birds as sentinels of environmental pollution. *EcoHealth* 1:263–274.

Burnham KP, Anderson DR. 2002. *Model Selection and Multi-Model Inference: A Practical Information-Theoretic Approach*, 2nd ed. Springer, New York, NY, USA.

Bustamante P, Lahaye V, Durnez C, Churlaud C, Caurant F. 2006. Total and organic Hg, concentrations in cephalopods from the North Eastern Atlantic waters: Influence of geographical origin and feeding ecology. *Sci Total Environ* 368:585–596.

Capone DG, Hutchins DA. 2013. Microbial biogeochemistry of coastal upwelling regimes in a changing ocean. *Nat Geosci* 6:711–717.

Carravieri A, Burthe SJ, De la Vega C, Yonehara Y, Daunt F, Newell MA, Jeffreys RM, Lawlor AJ, Hunt A, Shore RF, Pereira MG. 2020b. Interactions between environmental contaminants and gastrointestinal parasites: Novel insights from an integrative approach in a marine predator. *Environ Sci Technol* 54:8938–8948.

Carravieri A, Bustamante P, Churlaud C, Cherel Y. 2013. Penguins as bioindicators of mercury contamination in the Southern Ocean: Birds from the Kerguelen Islands as a case study. *Sci Total Environ* 454–455:141–148.

Carravieri A, Bustamante P, Churlaud C, Fromant A, Cherel Y. 2014c. Moulting patterns drive within-individual variations of stable isotopes and mercury in seabird body feathers: Implications for monitoring of the marine environment. *Mar Biol* 161:963–968.

Carravieri A, Bustamante P, Labadie P, Budzinski H, Chastel O, Cherel Y. 2020a. Trace elements and persistent organic pollutants in chicks of 13 seabird species from Antarctica to the subtropics. *Environ Int* 134:105225.

Carravieri A, Bustamante P, Tartu S, Meillère A, Labadie P, Budzinski H, Peluhet L, Barbraud C, Weimerskirch H, Chastel O, Cherel Y. 2014b. Wandering albatrosses document latitudinal variations in the transfer of persistent organic pollutants and mercury to Southern Ocean predators. *Environ Sci Technol* 48:14746–14755.

Carravieri A, Cherel Y, Blévin P, Brault-Favrou M, Chastel O, Bustamante P. 2014a. Mercury exposure in a large subantarctic avian community. *Environ Pollut* 190:51–57.

Carravieri A, Cherel Y, Brault-Favrou M, Churlaud C, Peluhet L, Labadie P, Budzinski H, Chastel O, Bustamante P. 2017. From Antarctica to the subtropics: Contrasted geographical concentrations of selenium, mercury, and persistent organic pollutants in skua chicks (*Catharacta* spp.). *Environ Pollut* 228:464–473.

Carravieri A, Cherel Y, Jaeger A, Churlaud C, Bustamante P. 2016. Penguins as bioindicators of mercury contamination in the southern Indian Ocean: Geographical and temporal trends. *Environ Pollut* 213:195–205.

Cherel Y, Barbraud C, Lahournat M, Jaeger A, Jaquemet S, Wanless RM, Phillips RA, Thompson DR, Bustamante P. 2018. Accumulate or eliminate? Seasonal mercury dynamics in albatrosses, the most contaminated family of birds. *Environ Pollut* 241:124–135.

Cherel Y, Fontaine C, Richard P, Labat J-P. 2010. Isotopic niches and trophic levels of myctophid fishes and their predators in the Southern Ocean. *Limnol Oceanogr* 55:324–332.

Cherel Y, Hobson KA. 2007. Geographical variation in carbon stable isotope signatures of marine predators: A tool to investigate their foraging areas in the Southern Ocean. *Mar Ecol Prog Ser* 329:281–287.

Cherel Y, Hobson KA, Bailleul F, Groscolas R. 2005. Nutrition, physiology, and stable isotopes: New information from fasting and molting penguins. *Ecology* 86:2881–2888.

Chikaraishi Y, Ogawa NO, Kashiyama Y, Takano Y, Suga H, Tomitani A, Miyashita H, Kitazato H, Ohkouchi N. 2009. Determination of aquatic food-web structure based on compound-specific nitrogen isotopic composition of amino acids. *Limnol Oceanogr Methods* 7:740–750.

Chouvelon T, Cresson P, Bouchoucha M, Brach-Papa C, Bustamante P, Crochet S, Marco-Miralles F, Thomas B, Knoery J. 2018. Oligotrophy as a major driver of mercury bioaccumulation in medium- to high-trophic level consumers: A marine ecosystem-comparative study. *Environ Pollut* 233:844–854.

Chouvelon T, Spitz J, Caurant F, Mèndez-Fernandez P, Autier J, Lassus-Débat A, Chappuis A, Bustamante P. 2012. Enhanced bioaccumulation of mercury in deep-sea fauna from the Bay of Biscay (north-east Atlantic) in relation to trophic positions identified by analysis of carbon and nitrogen stable isotopes. *Deep Sea Res Part I Oceanogr Res Pap* 65:113–124.

Chouvelon T, Spitz J, Cherel Y, Caurant F, Sirmel R, Mèndez-Fernandez P, Bustamante P. 2011. Inter-specific and ontogenic differences in $\delta^{13}C$ and $\delta^{15}N$ values and Hg and Cd concentrations in cephalopods. *Mar Ecol Prog Ser* 433:107–120.

Choy CA, Popp BN, Kaneko JJ, Drazen JC. 2009. The influence of depth on mercury levels in pelagic fishes and their prey. *Proc Natl Acad Sci USA* 106:13865–13869.

Chrystall L, Rumsby A. 2009. Mercury inventory for New Zealand 2008. New Zealand Ministry for the Environment Manatū Mō Te Taiao. [cited 2020 June 29]. Available from: https://www.mfe.govt.nz/sites/default/files/mercury-inventory-new-zealand-2008.pdf

Cipro CVZ, Cherel Y, Caurant F, Miramand P, Mendez-Fernandez P, Bustamante P. 2014. Trace elements in tissues of white-chinned petrels (*Procellaria aequinoctialis*) from Kerguelen waters, Southern Indian Ocean. *Polar Biol* 37:763–771.

Cline JD, Richards RA. 1972. Oxygen deficient conditions and nitrate reduction in the eastern tropical North Pacific Ocean. *Limnol Oceanogr* 17:885–900.

Codispoti LA, Christensen JP. 1985. Nitrification, denitrification and nitrous oxide cycling in the eastern tropical South Pacific Ocean. *Mar Chem* 16:277–300.

Cossa D, Heimbürger LE, Lannuzel D, Rintoul SR, Butler ECV, Bowie AR, Averty B, Watson RJ, Remenyi T. 2011. Mercury in the Southern Ocean. *Geochim Cosmochim Acta* 75:4037–4052.

Costantini D, Meillère A, Carravieri A, Lecomte V, Sorci G, Faivre B, Weimerskirch H, Bustamante P, Labadie P, Budzinski H, Chastel O. 2014. Oxidative stress in relation to reproduction, contaminants, gender and age in a long-lived seabird. *Oecologia* 175:1107–1116.

Croxall JP, Prince PA. 1980. Food, feeding ecology and ecological segregation of seabirds at South Georgia. *Biol J Linn Soc* 14:103–131.

Cruz JB, Lalas C, Jillett JB, Kitson JC, Lyver PO'B, Imber M, Newman JE, Moller H. 2001. Prey spectrum of breeding sooty shearwaters (*Puffinus griseus*) in New Zealand. *New Zealand J Mar Freshwater Res* 35:817–829.

DeNiro MJ, Epstein S. 1977. Mechanism of carbon isotope fractionation associated with lipid synthesis. *Science* 197:261–263.

DeNiro MJ, Epstein S. 1981. Influence of diet on the distribution of nitrogen isotopes in animals. *Geochim Cosmochim Acta* 45:341–351.

Dietz R, Riget F, Cleemann M, Aarkrog A, Johansen P, Hansen JC. 2000. Comparison of contaminants from different trophic levels and ecosystems. *Sci Total Environ* 245:221–231.

Eagles-Smith CA, Silbergeld EK, Basu N, Bustamante P, Diaz-Barriga F, Hopkins WA, Kidd KA, Nyland JF. 2018. Modulators of mercury risk to wildlife and humans in the context of rapid global change. *Ambio* 47:170–197.

Eisler R. 1987. Mercury hazards to fish, wildlife, and invertebrates: A synoptic review. *Biol Reprod* 85:1–10.

Elliott KH, Elliott JE. 2016. Origin of sulfur in diet drives spatial and temporal mercury trends in seabird eggs from Pacific Canada 1968–2015. *Environ Sci Technol* 50:13380–13386.

Evers DC, Savoy LJ, DeSorbo CR, Yates DE, Hanson W, Taylor KM, Siegel LS, Cooley JH Jr, Bank MS, Major A, Munney K, Mower BF, Vogel HS, Schoch N, Pokras M, Goodale MW, Fair J. 2008. Adverse effects from environmental mercury loads on breeding common loons. *Ecotoxicology* 17:69–81.

Fitzgerald WF, Engstrom DR, Mason RP, Nater EA. 1998. The case for atmospheric mercury contamination in remote areas. *Environ Sci Technol* 32:1–7.

Fitzgerald WF, Lamborg CH, Hammerschmidt CR. 2007. Marine biogeochemical cycling of mercury. *Chem Rev* 107:641–662.

Fromant A, Carravieri A, Bustamante P, Labadie P, Budzinski H, Peluhet L, Churlaud C, Chastel O, Cherel Y. 2016. Wide range of metallic and organic contaminants in various tissues of the Antarctic prion, a planktonophagous seabird from the Southern Ocean. *Sci Total Environ* 544:754–764.

Fuenzalida R, Schneider W, Garcés-Vargas J, Bravo L, Lange C. 2009. Vertical and horizontal extension of the oxygen minimum zone in the eastern South Pacific Ocean. *Deep Sea Res Part 2 Top Stud Oceanogr* 56:992–1003.

Furness RW, Muirhead SJ, Woodburn M. 1986. Using bird feathers to measure mercury in the environment: Relationships between mercury content and moult. *Mar Pollut Bull* 17:27–30.

Gagné TO, Johnson EM, Hyrenbach KD, Hagemann ME, Bass OL, MacDonald M, Peck B, Van Houtan KS. 2019. Coupled trophic and contaminant analysis in seabirds through space and time. *Environ Res Commun* 1:111006.

Giglioli HH, Salvadori T. 1869. On some new Procellariidae collected during a voyage round the world in 1865–1868 in H.I.M.S. "Magenta". *Ibis* (Lond 1859) 5:61–68. In Bourne WRP. 1964. The relationship between the Magenta petrel and the Chatham Island Taiko. *Notornis* 11:139–144.

Gilbertson M, Elliott JE, Peakall DB. 1987. Seabirds as indicators of marine pollution. *International Council for Bird Preservation Tech Pub* 6:231–248.

Gochfeld M. 1980. Mercury levels in some seabirds of the Humboldt Current, Peru. *Environ Pollut* 22:197–205.

Gochfeld M, Gochfeld DJ, Minton D, Murray BG Jr, Pyle P, Seto N, Smith D, Burger J. 1999. Metals in feathers of Bonin petrel, Christmas shearwater, wedge-tailed shearwater, and red-tailed tropicbird in the Hawaiian Islands, Northern Pacific. *Environ Monit Assess* 59:343–358.

Goutte A, Barbraud C, Herzke D, Bustamante P, Angelier F, Tartu S, Clement-Chastel C, Moe B, Bech C, Gabrielsen GW, Bustnes JO, Chastel O. 2015. Survival rate and breeding outputs in a high Arctic seabird exposed to legacy persistent organic pollutants and mercury. *Environ Pollut* 200:1–9.

Goutte A, Barbraud C, Meillère A, Carravieri A, Bustamante P, Labadie P, Budzinski H, Delord K, Cherel Y, Weimerskirch H, Chastel O. 2014. Demographic consequences of heavy metals and persistent organic pollutants in a vulnerable long-lived bird, the wandering albatross. *Proc Roy Soc Lond B Biol Sci* 281:20133313.

Grecian WJ, Taylor GA, Loh G, McGill RAR, Miskelly CM, Phillips RA, Thompson DR, Furness RW. 2016. Contrasting migratory responses of two closely related seabirds to long-term climate change. *Mar Ecol Prog Ser* 559:231–242.

Gross WB, Siegel HS. 1983. Evaluation of the heterophil/lymphocyte ratio as a measure of stress in chickens. *Avian Dis* 27:972–979.

Hawkey CM, Dennett TB, Peirce MA. 1989. *A Colour Atlas of Comparative Veterinary Haematology: Normal and Abnormal Blood Cells in Mammals, Birds and Reptiles*. Wolfe, London, UK.

Heather BD, Robertson HA. 2005. *The Field Guide to the Birds of New Zealand*. Penguin NZ, Auckland, New Zealand.

Hebert CE, Popp BN, Fernie KJ, Ka'apu-Lyons C, Rattner BA, Wallsgrove N. 2016. Amino acid specific stable nitrogen isotope values in avian tissues: Insights from captive American kestrels and wild herring gulls. *Environ Sci Technol* 50:12928–12937.

Heinz GH, Hoffman DJ, Klimstra JD, Stebbins KR, Kondrad SL, Erwin CA. 2009. Species differences in the sensitivity of avian embryos to methylmercury. *Arch Environ Contam Toxicol* 56:129–138.

Hoen DK, Kim SL, Hussey NE, Wallsgrove NJ, Drazen JC, Popp BN. 2014. Amino acid ^{15}N trophic enrichment factors of four large carnivorous fishes. *J Exp Mar Biol Ecol* 453:76–83.

Hsu-Kim H, Kucharzyk KH, Zhang T, Deshusses MA. 2013. Mechanisms regulating mercury bioavailability for methylating microorganisms in the aquatic environment: A critical review. *Environ Sci Technol* 47:2441–2456.

Imber MJ. 1981. Diets of storm petrels *Pelagodroma* and *Garrodia* and of prions *Pachyptila* (Procellariiformes): Ecological separation and bill morphology. *Proceedings*, Symposium on birds of the sea and shore, Cooper J ed, Cape Town: African Seabird Group, Cape Town, South Africa, November 19–21, 1979, pp 63–88.

Imber MJ. 1985. Origins, phylogeny and taxonomy of the gadfly petrels *Pterodroma* spp. *Ibis* (Lond 1859) 127:197–229.

Imber MJ, Crockett DE, Gordon AH, Best HA, Douglas ME, Cotter RN. 1994. Finding the burrows of Chatham Island Taiko *Pterodroma magentae* by radio telemetry. *Notornis* 41(Suppl):69–96.

Inger R, Bearhop S. 2008. Applications of stable isotope analyses to avian ecology. *Ibis* (Lond 1859) 150:447–461.

Jackson A, Inger R, Pamell AC, Bearhop S. 2011. Comparing isotopic niche widths among and within communities: SIBER—Stable Isotope Bayesian Ellipses in R. *J Anim Ecol* 80:595–602.

Jaeger A, Lecomte VJ, Weimerskirch H, Richard P, Cherel Y. 2010. Seabird satellite tracking validates the use of latitudinal isoscapes to depict predators' foraging areas in the Southern Ocean. *Rapid Commun Mass Spectrom* 24:3456–3460.

Johnson JB, Omland KS. 2004. Model selection in ecology and evolution. *Trends Ecol Evol* 19:101–108.

Kitson JC, Cruz JB, Lalas C, Jillett JB, Newman J, Lyver PO'B. 2000. Inter-annual variations in the diet of breeding sooty shearwaters (*Puffinus griseus*). *N Z J Zool* 27:347–355.

Klages NTW, Cooper J. 1992. Bill morphology and diet of a filter-feeding seabird: The broad-billed prion *Pachyptila vittata* at South Atlantic Gough Island. *J Zool* (Lond) 227:385–396.

Kojadinovic J, Bustamante P, Churlaud C, Cosson RP, Le Corre M. 2007. Mercury in seabird feathers: Insight on dietary habits and evidence for exposure levels in the western Indian Ocean. *Sci Total Environ* 384:194–204.

Kojadinovic J, Potier M, Le Corre M, Cosson RP, Bustamante P. 2006. Mercury content in commercial pelagic fish and its risk assessment in the Western Indian Ocean. *Sci Total Environ* 366:688–700.

Lamborg CH, Hammerschmidt CR, Bowman KL, Swarr GJ, Munson KM, Ohnemus DC, Lam PJ, Heimburger L-E, Rijkenberg MJA, Saito MA.

2014. A global ocean inventory of anthropogenic mercury based on water column measurements. *Nature* 512:65–68.

Lavoie RA, Jardine TD, Chumchal MM, Kidd KA, Campbell LM. 2013. Biomagnification of mercury in aquatic food webs: A worldwide meta-analysis. *Environ Sci Technol* 47:13385–13394.

Lewis SA, Furness RW. 1991. Mercury accumulation and excretion in laboratory reared black-headed gull *Larus ridibundus* chicks. *Arch Environ Contam Toxicol* 21:316–320.

Lobato E, Moreno J, Merino S, Sanz J, Arriero E. 2005. Haematological variables are good predictors of recruitment in nestling pied flycatchers (*Ficedula hypoleuca*). *Écoscience* 12:27–34.

Lock JW, Thompson DR, Furness RW, Bartle JA. 1992. Metal concentrations in seabirds of the New Zealand region. *Environ Pollut* 75:289–300.

Lyver PO'B, Aldridge SP, Gormley AM, Gaw S, Webb S, Buxton RT, Jones CJ. 2017. Elevated mercury concentrations in the feathers of grey-faced petrels (*Pterodroma gouldi*) in New Zealand. *Mar Pollut Bull* 119:195–203.

Martinez del Rio C, Wolf N, Carleton SA, Gannes LZ. 2009. Isotopic ecology ten years after a call for more laboratory experiments. *Biol Rev* 84:91–111.

McClelland JW, Montoya JP. 2002. Trophic relationships and the nitrogen isotopic composition of amino acids in plankton. *Ecology* 83:2173–2180.

McMahon KW, Hamady LL, Thorrold SR. 2013. A review of ecogeochemistry approaches to estimating movements of marine animals. *Limnol Oceanogr* 58:697–714.

McMahon KW, McCarthy MD. 2016. Embracing variability in amino acid δ^{15}N fractionation: Mechanisms, implications, and applications for trophic ecology. *Ecosphere* 7:e01511.

McMahon KW, Polito MJ, Abel S, McCarthy MD, Thorrold SR. 2015. Carbon and nitrogen isotope fractionation of amino acids in an avian marine predator, the gentoo penguin (*Pygoscelis papua*). *Ecol Evol* 5:1278–1290.

Minami H, Ogi H. 1997. Determination of migratory dynamics of the sooty shearwater in the Pacific using stable carbon and nitrogen isotope analysis. *Mar Ecol Prog Ser* 158:249–256.

Monteiro LR, Costa V, Furness RW, Santos RS. 1996. Mercury concentrations in prey fish indicate enhanced bioaccumulation in mesopelagic environments. *Mar Ecol Prog Ser* 141:21–25.

Monteiro LR, Furness RW. 1995. Seabirds as monitors of mercury in the marine environment. *Water Air Soil Pollut* 80:851–870.

Monteiro LR, Furness RW. 2001. Kinetics, dose-response, excretion, and toxicity of methylmercury in free-living Cory's shearwater chicks. *Environ Toxicol Chem* 20:1816–1823.

Ochoa-Acuña H, Sepúlveda MS, Gross TS. 2002. Mercury in feathers from Chilean birds: Influence of location, feeding strategy, and taxonomic affiliation. *Mar Pollut Bull* 44:340–349.

Pacyna EG, Pacyna JM, Steenhuisen F, Wilson S. 2006. Global anthropogenic mercury emission inventory for 2000. *Atmos Environ* 40:4048–4063.

Payne MR, Prince PA. 1979. Identification and breeding biology of the diving petrels *Pelecanoides georgicus* and *P. urinatrix exsul* at South Georgia. *N Z J Zool* 6:299–318.

Pirrone N, Cinnirella S, Feng X, Finkelman RB, Friedli HR, Leaner J, Mason R, Mukherjee AB, Stracher GB, Streets DG, Telmer K. 2010. Global mercury emissions to the atmosphere from anthropogenic and natural sources. *Atmos Chem Phys* 10:5951–5964.

Post DM. 2002. Using stable isotopes to estimate trophic position: Models, methods, and assumptions. *Ecology* 83:703–718.

Post DM, Layman CA, Albrey Arrington D, Takimoto G, Quattrochi J, Montana CG. 2007. Getting to the fat of the matter: Models, methods and assumptions for dealing with lipids in stable isotope analyses. *Oecologia* 152:179–189.

Quillfeldt P, Masello JF. 2020. Compound-specific stable isotope analyses in Falkland Islands seabirds reveal seasonal changes in trophic positions. *BMC Ecol* 20:21.

Quillfeldt P, Thorn S, Richter B, Nabte M, Coria N, Masello JF, Massaro M, Neves VC, Libertelli M. 2017. Testing the usefulness of hydrogen and compound-specific stable isotope analyses in seabird feathers: A case study in two sympatric Antarctic storm-petrels. *Mar Biol* 164:192.1–192.7.

Quillfeldt PQ, McGill RAR, Masello JF, Weiss F, Strange IJ, Brickle P, Furness RW. 2008. Stable isotope analysis reveals sexual and environmental variability and individual consistency in foraging of thin-billed prions. *Mar Ecol Prog Ser* 373:137–148.

R Development Core Team. 2019. *A Language and Environment for Statistical Computing*. R Foundation for Statistical Computing, Vienna, Austria. [cited 2020 May 2]. Available from: https://www.R-project.org/

Rabenstein DL. 1978a. The aqueous solution chemistry of methylmercury and its complexes. *Acc Chem Res* 11:100–107.

Rabenstein DL. 1978b. The chemistry of methylmercury toxicology. *J Chem Educ* 55:292–296.

Ramos R, Ramírez F, Jover L. 2013. Trophodynamics of inorganic pollutants in a wide-range feeder: The relevance of dietary inputs and bio-magnification in the yellow-legged gull (*Larus michahellis*). *Environ Pollut* 172:235–242.

Rayner MJ, Taylor GA, Gummer HD, Phillips RA, Sagar PM, Shaffer SA, Thompson DR. 2012. The breeding cycle, year-round distribution and activity patterns of the endangered Chatham petrel (*Pterodroma axillaris*). *Emu* 112:107–116.

Reid K, Coxall JP, Edwards TM, Hill HJ, Prince PA. 1997. Diet and feeding ecology of the diving petrels *Pelecanoides georgicus* and *P. urinatrix* at South Georgia. *Polar Biol* 17:17–24.

Renedo M, Bustamante P, Cherel Y, Pedrero Z, Tessier E, Amouroux D. 2020. A "seabird-eye" on mercury stable isotopes and cycling in the Southern Ocean. *Sci Total Environ* 742:140499.

Renedo M, Bustamante P, Tessier E, Pedrero Z, Cherel Y, Amouroux D. 2017. Assessment of mercury speciation in feathers using species-specific isotope dilution analysis. *Talanta* 174:100–110.

Renedo M, Pedredo Z, Amouroux D, Cherel Y, Bustamante P. 2021. Mercury isotopes of key tissues document mercury metabolic processes in sea-birds. *Chemosphere* 263:127777.

Richdale LE. 1944. The parara or broad-billed prion *Pachyptila vittata* (Gmelin). *Emu* 43:191–217.

Ridoux V. 1994. The diets and dietary segregation of seabirds at the Sub-antarctic Crozet Islands. *Mar Ornithol* 22:1–64.

Saiz-Lopez A, Sitkiewicz SP, Roca-Sanjuán D, Oliva-Enrich JM, Dávalos JZ, Notario R, Jiskra M, Xu Y, Wang F, Thackray CP, Sunderland EM, Jacob DJ, Travnikov O, Cuevas CA, Acuña AU, Rivero D, Plane JMC, Kinnison DE, Sonke JE. 2018. Photoreduction of gaseous oxidized mercury changes global atmospheric mercury speciation, transport and deposition. *Nat Commun* 9:4796.

Scheuhammer AM. 1987. The chronic toxicity of aluminium, cadmium, mercury, and lead in birds: A review. *Environ Pollut* 46:263–295.

Schumann N, Arnould JPY, Dann P. 2008. Diet of common diving-petrels (*Pelecanoides urinatrix urinatrix*) in Southeastern Australia during chick rearing. *Waterbirds Int J Waterbird Biol* 31:620–624.

Shaffer SA, Weimerskirch H, Scott D, Pinaud D, Thompson DR, Sagar PM, Moller H, Taylor GA, Foley DG, Tremblay Y, Costa DP. 2009. Spatio-temporal habitat use by breeding sooty shearwaters *Puffinus griseus*. *Mar Ecol Prog Ser* 391:209–220.

Spalding MG, Frederick PC, McGill HC, Bouton SN, Richey LJ, Schumacher IM, Blackmore CGM, Harrison J. 2000. Histologic, neurologic, and im-munologic effects of methylmercury in captive great egrets. *J Wildl Dis* 36:423–435.

Spear LB, Ainley DG. 2007. Storm-petrels of the eastern Pacific Ocean: Species assembly and diversity along marine habitat gradients. *Ornithol Monogr* 62:1–77.

Stewart F, Phillips R, Bartle A, Craig J, Shooter D. 1999. Influence of phy-logeny, diet, moult schedule and sex on heavy metal concentrations in New Zealand Procellariiformes. *Mar Ecol Prog Ser* 178:295–305.

Swartz W, Rashid Sumaila U, Watson R, Pauly D. 2010. Sourcing seafood for the three major markets: The EU, Japan and the USA. *Mar Policy* 34:1366–1373.

Tan SW, Meiller JC, Mahaffey KR. 2009. The endocrine effects of mercury in humans and wildlife. *Crit Rev Toxicol* 39:228–269.

Tartu S, Angelier F, Wingfield JC, Bustamante P, Labadie P, Budzinski H, Weimerskirch H, Bustnes JO, Chastel O. 2015. Corticosterone, prolactin and egg neglect behavior in relation to mercury and legacy POPs in a long-lived Antarctic bird. *Sci Total Environ* 505:180–188.

Tartu S, Goutte A, Bustamante P, Angelier F, Moe B, Clément-Chastel C, Bech C, Gabrielsen GW, Bustnes JO, Chastel O. 2013. To breed or not to breed: Endocrine response to mercury contamination by an Arctic seabird. *Biol Lett* 9:20130317.

Tavares S, Xavier JC, Phillips RA, Pereira ME, Pardal MA. 2013. Influence of age, sex and breeding status on mercury accumulation patterns in the wandering albatross *Diomedea exulans*. *Environ Pollut* 181:315–320.

Taylor GA. 2008. Maximum dive depths of eight New Zealand Procellar-iiformes, including *Pterodroma* species. *Pap Proc R Soc Tasm* 142:89–97.

Taylor GA. 2013. Chatham Island taiko. New Zealand birds online. In Miskelly CM (ed.). [cited 2020 June 1]. Available from: http://www.nzbirdsonline.org.nz/species/chatham-island-taiko

Taylor G, Cockburn S, Palmer D, Liddy P. 2012. Monitoring breeding activity of Chatham Island taiko (*Pterodroma magentae*) using PIT tag recorders. *N Z J Ecol* 36:425–432.

Taylor GA, Elliott GP, Walker KJ, Bose S. 2020. Year-round distribution, breeding cycle, and activity of white-headed petrels (*Pterodroma lessonii*) nesting on Adams Island, Auckland Islands. *Notornis* 67:369–386.

Thompson DR, Furness RW, Lewis SA. 1993. Temporal and spatial variation in mercury concentrations in some albatrosses and petrels from the sub-Antarctic. *Polar Biol* 13:239–244.

Thompson DR, Furness RW, Monteiro LR. 1998. Seabirds as biomonitors of mercury inputs to epipelagic and mesopelagic marine food chains. *Sci Total Environ* 213:299–305.

Thompson DR, Stewart FM, Furness RW. 1990. Using seabirds to monitor mercury in marine environments: The validity of conversion ratios for tissue comparisons. *Mar Pollut Bull* 21:339–342.

Vander Zanden MJ, Clayton MK, Moody EK, Solomon CT, Weidel BC. 2015. Stable isotope turnover and half-life in animal tissues: A literature syn-thesis. *PLoS One* 10:e0116182.

Villar E, Cabrol L, Heimbürger-Boavida L-E. 2020. Widespread microbial mercury methylation genes in the global ocean. *Environ Microbiol Rep* 12:277–287.

Vleck CM, Vertalino N, Vleck D, Bucher TL. 2000. Stress, corticosterone and heterophil to lymphocyte ratios in free-living Adélie penguins. *Condor* 102:392–400.

Walker CH, Sibly RM, Hopkin SP, Peakall DB. 2012. *Principles of Ecotox-icology*, 4th ed. CRC, Boca Raton, FL, USA.

Walsh R, He S, Yarnes CT. 2014. Compound-specific $\delta^{13}C$ and $\delta^{15}N$ analysis of amino acids: A rapid, chloroformate-based method for ecological studies. *Rapid Commun Mass Spectrom* 28:96–108.

Weimerskirch H. 1998. How can a pelagic seabird provision its chick when relying on a distant food resource? Cyclic attendance at the colony, foraging decision and body condition in sooty shearwaters. *J Anim Ecol* 67:99–109.

Weissberg BG, Rohde AG. 1978. Mercury in some New Zealand geothermal discharges. *NZ J Sci* 21:365–369.

Weissberg BG, Zobel MGR. 1973. Geothermal mercury pollution in New Zealand. *Bull Environ Contam Toxicol* 9:148–155.

Wolfe MF, Schwarzbach S, Sulaiman RA. 1998. Effects of mercury on wild-life: A comprehensive review. *Environ Toxicol Chem* 17:146–160.

Yarnes CT, Herszage J. 2017. The relative influence of derivatization and normalization procedures on the compound-specific stable isotope analysis of nitrogen in amino acids. *Rapid Commun Mass Spectrom* 31:693–704.